U.S. Department
of Transportation

Federal Railroad
Administration

Office of Research,
Development and Technology
Washington, DC 20590

Wireless Digital Train Line for Passenger Trains – Phase 3

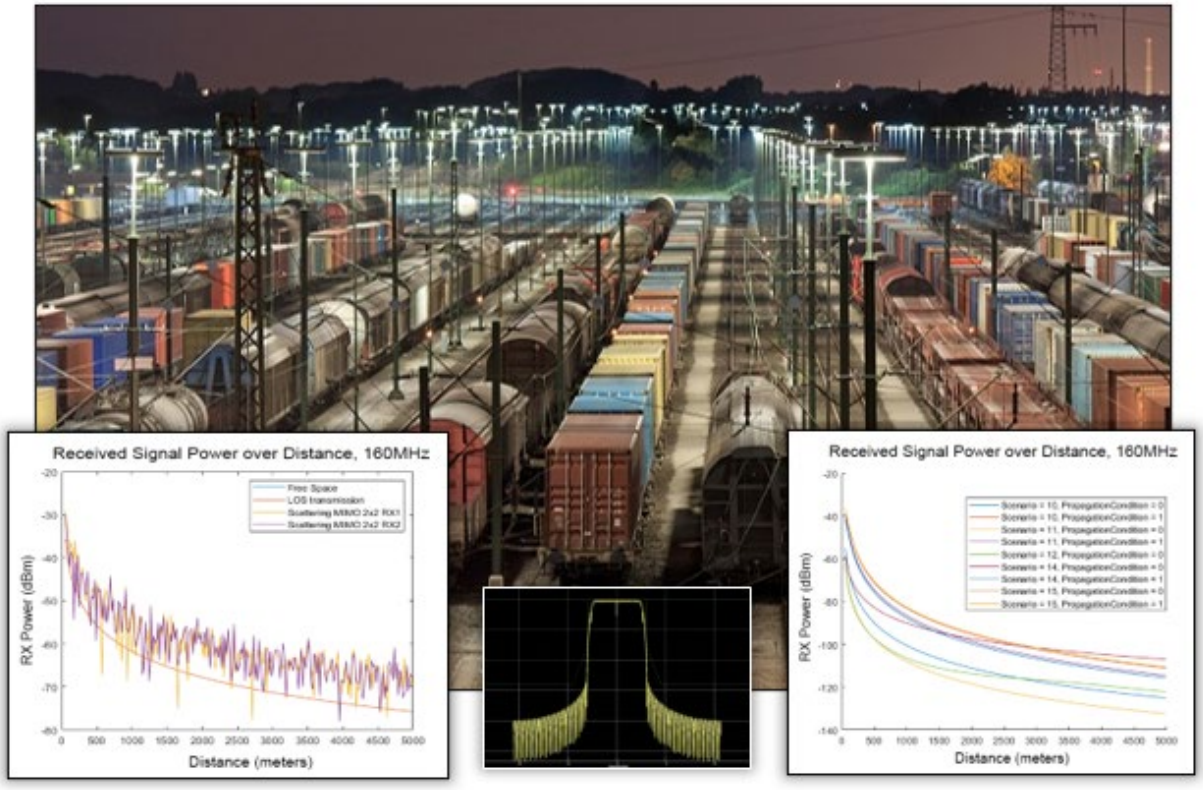

DOT/FRA/ORD-23/06

Final Report | February 2023

REPORT DOCUMENTATION PAGE

Form Approved
OMB No. 0704-0188

1. REPORT DATE *(DD-MM-YYYY)*	**2. REPORT TYPE**	**3. DATES COVERED** *(From - To)*
February 10, 2023	Technical Report	August 2020–July 2022

4. TITLE AND SUBTITLE
Wireless Digital Train Line for Passenger Trains – Phase 3

5a. CONTRACT NUMBER
FR-RRD-0086-20-01-00

5b. GRANT NUMBER

5c. PROGRAM ELEMENT NUMBER

6. AUTHOR(S)
Hamid Sharif: 0000-0001-6229-2043
Michael Hempel: 0000-0002-7091-8349

5d. PROJECT NUMBER

5e. TASK NUMBER

5f. WORK UNIT NUMBER

7. PERFORMING ORGANIZATION NAME(S) AND ADDRESS(ES)
Board of Regents of the University of Nebraska for the University of Nebraska-Lincoln
3835 Holdrege Street
Lincoln, Nebraska 68583

8. PERFORMING ORGANIZATION REPORT NUMBER

9. SPONSORING/MONITORING AGENCY NAME(S) AND ADDRESS(ES)
U.S. Department of Transportation
Federal Railroad Administration
Office of Railroad Policy and Development
Office of Research, Development and Technology
Washington, DC 20590

10. SPONSOR/MONITOR'S ACRONYM(S)

11. SPONSOR/MONITOR'S REPORT NUMBER(S)
DOT/FRA/ORD-23/06

12. DISTRIBUTION/AVAILABILITY STATEMENT
This document is available to the public through the FRA website.

13. SUPPLEMENTARY NOTES
COR: Tarek Omar

14. ABSTRACT

In an extensive third phase of a Federal Railroad Administration-funded research project running from August 2020 through July 2022, a team at the Advanced Telecommunications Engineering Laboratory at the University of Nebraska-Lincoln designed, developed, and evaluated wireless communications architectures for rail services in North America, with a focus on high-speed rail services. During this phase, the team focused on mitigating a significant challenge, not only in the rail industry but in fact across all sectors: radio frequency (RF) spectrum scarcity. RF spectrum resources are a necessity for any wireless solution, and with the rapid proliferation of wireless services and applications in all aspects of daily life and society, RF resources are becoming overused and expensive to license. Therefore, the team studied RF spectrum already owned by the rail industry, but that may be abandoned, underused, or used only for legacy applications. Such bands are ideal candidates for modernization and re-use.

15. SUBJECT TERMS
Digital train line, wireless connectivity, WiDTL, user/control plane, high-speed rail, passenger rail service, 160MHz, performance evaluation, computer simulation

16. SECURITY CLASSIFICATION OF:			**17. LIMITATION OF ABSTRACT**	**18. NUMBER OF PAGES**	**19a. NAME OF RESPONSIBLE PERSON**
a. REPORT	**b. ABSTRACT**	**c. THIS PAGE**			**19b. TELEPHONE NUMBER** *(Include area code)*
Unclassified	Unclassified	Unclassified		68	

Standard Form 298 (Rev. 8/98)
Prescribed by ANSI Std. Z39.18

METRIC/ENGLISH CONVERSION FACTORS

ENGLISH TO METRIC	METRIC TO ENGLISH
LENGTH (APPROXIMATE)	**LENGTH (APPROXIMATE)**
1 inch (in) = 2.5 centimeters (cm)	1 millimeter (mm) = 0.04 inch (in)
1 foot (ft) = 30 centimeters (cm)	1 centimeter (cm) = 0.4 inch (in)
1 yard (yd) = 0.9 meter (m)	1 meter (m) = 3.3 feet (ft)
1 mile (mi) = 1.6 kilometers (km)	1 meter (m) = 1.1 yards (yd)
	1 kilometer (km) = 0.6 mile (mi)
AREA (APPROXIMATE)	**AREA (APPROXIMATE)**
1 square inch (sq in, in^2) = 6.5 square centimeters (cm^2)	1 square centimeter (cm^2) = 0.16 square inch (sq in, in^2)
1 square foot (sq ft, ft^2) = 0.09 square meter (m^2)	1 square meter (m^2) = 1.2 square yards (sq yd, yd^2)
1 square yard (sq yd, yd^2) = 0.8 square meter (m^2)	1 square kilometer (km^2) = 0.4 square mile (sq mi, mi^2)
1 square mile (sq mi, mi^2) = 2.6 square kilometers (km^2)	10,000 square meters (m^2) = 1 hectare (ha) = 2.5 acres
1 acre = 0.4 hectare (he) = 4,000 square meters (m^2)	
MASS - WEIGHT (APPROXIMATE)	**MASS - WEIGHT (APPROXIMATE)**
1 ounce (oz) = 28 grams (gm)	1 gram (gm) = 0.036 ounce (oz)
1 pound (lb) = 0.45 kilogram (kg)	1 kilogram (kg) = 2.2 pounds (lb)
1 short ton = 2,000 pounds (lb) = 0.9 tonne (t)	1 tonne (t) = 1,000 kilograms (kg) = 1.1 short tons
VOLUME (APPROXIMATE)	**VOLUME (APPROXIMATE)**
1 teaspoon (tsp) = 5 milliliters (ml)	1 milliliter (ml) = 0.03 fluid ounce (fl oz)
1 tablespoon (tbsp) = 15 milliliters (ml)	1 liter (l) = 2.1 pints (pt)
1 fluid ounce (fl oz) = 30 milliliters (ml)	1 liter (l) = 1.06 quarts (qt)
1 cup (c) = 0.24 liter (l)	1 liter (l) = 0.26 gallon (gal)
1 pint (pt) = 0.47 liter (l)	
1 quart (qt) = 0.96 liter (l)	
1 gallon (gal) = 3.8 liters (l)	
1 cubic foot (cu ft, ft^3) = 0.03 cubic meter (m^3)	1 cubic meter (m^3) = 36 cubic feet (cu ft, ft^3)
1 cubic yard (cu yd, yd^3) = 0.76 cubic meter (m^3)	1 cubic meter (m^3) = 1.3 cubic yards (cu yd, yd^3)
TEMPERATURE (EXACT)	**TEMPERATURE (EXACT)**
[(x-32)(5/9)] °F = y °C	[(9/5) y + 32] °C = x °F

QUICK INCH - CENTIMETER LENGTH CONVERSION

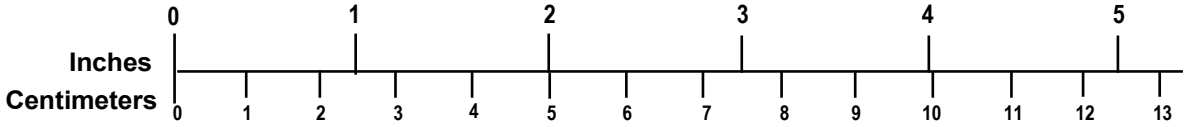

QUICK FAHRENHEIT - CELSIUS TEMPERATURE CONVERSIO

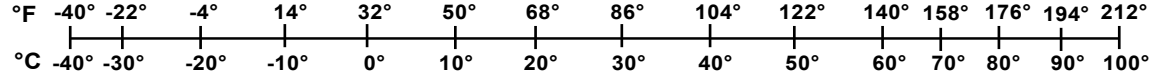

For more exact and or other conversion factors, see NIST Miscellaneous Publication 286, Units of Weights and Measures. Price $2.50 SD Catalog No. C13 10286

Updated 6/17/98

Acknowledgements

The research team would like to thank the stakeholders in this research study. For freight rail, the Association of American Railroad's (AAR's) Locomotive Committee formed the Locomotive Consist Control (LCC) Technical Advisory Group (TAG); for passenger rail, the effort was directed through the Next Generation Equipment Committee (NGEC). The team would like to express sincere thanks to both groups for their efforts.

Contents

Illustrations

Tables

Executive Summary

In an extensive third phase of a Federal Railroad Administration (FRA)-funded research project running from August 2020 through July 2022, a team at the Advanced Telecommunications Engineering Laboratory (TEL) at the University of Nebraska-Lincoln designed, developed, and evaluated wireless communications architectures for rail services in North America, with a focus on high-speed rail services.

During this phase, the team focused on mitigating a significant challenge, not only in the rail industry but across all sectors: radio frequency (RF) spectrum scarcity. RF spectrum resources are a necessity for any wireless solution, but with the rapid proliferation of wireless services and applications in all aspects of daily life and society, RF resources are becoming overused and expensive to license. Therefore, the team studied RF spectrum already owned by the rail industry, but that may be abandoned, underused, or used only for legacy applications. Such bands are ideal candidates for modernization and re-use.

The team first surveyed all RF resources owned or in use by the rail industry in North America and identified candidate RF bands. Researchers studied their regulatory requirements and constraints and surveyed tools to help evaluate operations in these frequency bands.

Researchers identified the 160 MHz band as the most suitable candidate for a case study effort. The team then studied different transceiver architectures, developed a full protocol stack on top of this architecture, and evaluated its performance metrics from a variety of perspectives.

The research team found the 160 MHz band to be compelling both for new applications and as an additional resource to alleviate pressure on existing applications such as the 220 MHz Positive Train Control (PTC) deployments in high-density areas such as the Chicago area or the Northeast Corridor.

In a subsequent phase of study, researchers plan to develop a universal software radio framework using the 160 MHz architecture as a case study implementation, and then conduct extensive field testing to accelerate the transition of this solution into various rail services and applications.

1. Introduction

In Phase 3 of a Federal Railroad Administration (FRA)-funded research project running from August 2020 through July 2022, a team at the Advanced Telecommunications Engineering Laboratory (TEL) at the University of Nebraska-Lincoln designed, developed, and evaluated wireless communications architectures for different rail applications and services such as high-speed rail, Wireless Digital Trainline (WiDTL), and Positive Train Control (PTC).

1.1 Background

A unique challenge for the rail industry in its pursuit of increasing wireless services is the need for more and more spectrum resources to be available to them across the entire operating arena. Wireless resources in general are increasingly scarce, expensive, or fragmented regionally.

Since it is becoming harder and harder to locate available radio frequency (RF) resources for rail industry applications, railroads are exploring the use of RF bands used in the past but then abandoned, or bands that are not currently used efficiently. Such bands have the potential to reinvigorate the drive toward modern wireless applications, particularly when coupled with innovative RF solutions such as Cognitive Radios that help to make RF spectrum use far more dynamic and efficient than current technologies.

One RF band that has seen particular interest from the rail industry is 160 MHz. This is a band currently used by railroads but fragmented across the industry and across the continent. This band also suffers from a relatively high channelization into small 25 kHz channels. These factors have limited interest in its use by modern rail applications, but with the renewed interest in this band comes the need for a comprehensive evaluation of its RF propagation and performance characteristics.

1.2 Objectives

The focus of this project phase's research effort was to explore the properties and capabilities of the 160 MHz RF band and its suitability for a variety of applications, including WiDTL. Another key goal was to explore if 160 MHz could alleviate the pressure on the 220 MHz PTC band in highly congested areas such as the Chicago metro or the Northeast Corridor. Finally, researchers sought to identify other frequency bands that may be candidates for modern wireless applications.

1.3 Overall Approach

The team's approach to this research phase was to first establish the groundwork for the effort by conducting a review of the 160 MHz frequency band and reviewing related frequency bands of secondary interest considering Federal Communications Commission (FCC) regulatory restrictions and capabilities. Researchers then reviewed and evaluated several path loss prediction models for use in end-to-end transceiver design. Finally, the team designed a full protocol stack for the transceiver architecture and implemented an event-driven simulation platform to evaluate its performance metrics.

This effort sets the stage for the next phase of research, in which the team will focus on designing and implementing a universal software radio approach and using 160 MHz as a case study target. Researchers will then use the 160 MHz software radio platform for extensive field

testing to collect real-world performance data to accelerate this solution's technology transfer to various rail applications.

Throughout this entire process, the team reported research findings and progress to responsible industry groups and stakeholders.

1.4 Scope

In this work, the primary focus was on the evaluation of 160 MHz application requirements, regulator and technology constraints, the design of a modern 160 MHz-based RF transceiver architecture, and its modeling and simulation-driven evaluation. This process also aims to set the stage for similar studies of additional frequency bands to maximize the access and use of various bands already available to the railroads but no longer in active use or currently only supporting legacy applications. The team believes this modernization is the most cost-effective approach to widen RF spectrum usage and support current and future RF applications in the North American rail industry.

1.5 Organization of the Report

The next several sections describe all the core efforts related to the team's work to design, implement, and evaluate a new architecture and protocol stack for a 160 MHz wireless solution for rail applications and services. This includes outreach activities to the stakeholders in this effort (Section 2), a survey of available rail RF spectrum resources (Section 3), an RF propagation study for 160 MHz (Section 4), the study of modulation schemes for single-carrier and Orthogonal Frequency-Division Multiplexing (OFDM)-based transceivers (Sections 5 and 6), a study of Error Correction Coding schemes (Section 7), the review and evaluation of different RF Channel Models for propagation analysis (Section 8), and the resulting transceiver design and protocol stack performance evaluation (Sections 9 and 10).

2. Stakeholder Engagement and Industry Participation

For this research to be truly applicable to addressing rail industry issues, it is vital to include regular and frequent communications with all relevant parties. This includes a variety of domains, from the project sponsor to equipment manufacturers and rail service operators. Therefore, the team focused on engaging with these stakeholders.

2.1 Stakeholder Groups

For this project researchers identified two key groups and the primary stakeholders:

- For freight rail, the Association of American Railroad's (AAR's) Locomotive Committee formed the Locomotive Consist Control (LCC) Technical Advisory Group (TAG). LCC TAG is responsible for overseeing the efforts on the freight railroad industry side and ensuring compliance with 49 CFR Part 229, Subpart E.
- For passenger rail, the effort is directed through the Next Generation Equipment Committee (NGEC). The NGEC was created in response to the Passenger Rail Investment and Improvement Act of 2008, H.R.6003, where Title III Section 305 instructs Amtrak to "establish a Next Generation Corridor Equipment Pool Committee to design, develop specifications for, and procure standardized next-generation corridor equipment." [1, 2]

2.2 Meeting and Conference Call Participation

Each group organized weekly or biweekly conference calls to inform members of ongoing efforts and progress. Team representatives were invited to join these calls and report on the research progress. The team continued this engagement throughout the entire project phase.

This regular and frequent engagement with stakeholders was a key resource in the research study. Every two weeks, during the NGEC conference calls, the team provided updates to the committee on progress for this project phase. The team intends to continue engagement with these groups beyond the end of this project to contribute to their ongoing efforts.

3. Rail Industry Spectrum Survey

3.1 Overview

Research work began with an extensive survey of RF bands suitable for the project goals. The focus during this project phase was on the evaluation of sub-1 GHz RF frequency bands, and the team attempted to identify all suitable frequency bands, including the 160 MHz band that was the focus of this research.

The available spectrum is a finite resource, and in the United States is managed by the FCC, which is responsible for licensing frequency bands to different organizations for various applications, and increasingly to maximize the efficient use of scarce frequency resources. The complete chart of frequency bands allocated by the FCC can be seen in Figure 1.

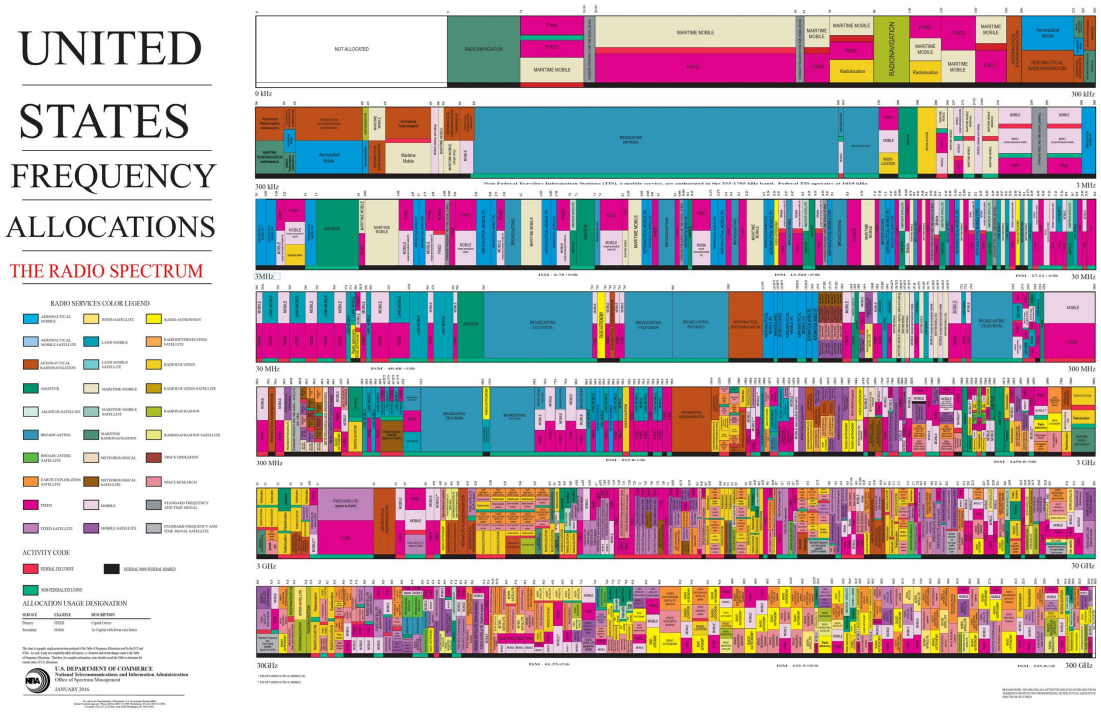

Figure 1. FCC Spectrum Allocation [4]

As shown in this figure, frequencies are broken down into bands that span from several kilohertz up to several megahertz. There are numerous frequency bands that are licensed to the rail industry. In some instances, the industry jointly licensed spectrum through AAR, which enables easier resource sharing among industry members. The FCC also imposes constraints on the use of RF bands, to better regulate adjacent band interference. Two of those factors, which play a crucial role for most applications, are [5]:

- the type of the user allowed to acquire the license on the frequency, and
- the maximum effective radiated power (ERP), depending on the antenna height, known as the Height Above Average Terrain (HAAT) factor.

The team investigated the frequencies licensed to the rail industry and explored their limitations based on available information. The available sub-gigahertz frequency bands for the rail industry can be generally categorized as shown in Table 1.

Table 1. Spectrum available to the rail industry [5]

Frequency Band (MHz)	Licensed Users
30-50	Utility, Railroads, Counties, Businesses
72-76	Mobile only – low power
150-174	Railroads, Businesses
217-222	Petroleum, Railroads, Businesses
450-470	Businesses, Petroleum, Public safety, Railroads – low power
896-902	Waiver Availability – limited
902-928	Railroads, Businesses

The respective license holders, and the intended applications for these bands, then specify additional parameters for the bands, such as channelization and modulation schemes. Some of these are standardized across the rail industry, which enables joint access and usage by railroads across North America, including Mexico and Canada.

3.2 Spectrum Analysis

The team investigated each of the bands shown in Table 1 in terms of their generic technical information, applications, and limitations.

3.2.1 Band: 30-50 MHz

The table shows that many of these bands are not licensed only to the rail industry; other industries have competed for these licenses and own them in various places across the country. One such example is the highly sought-after 30-50 MHz band, known as the "VHF low" band. The departments of energy, defense and interior are interested in this band for several uses, including tactical communication using the single channel ground and airborne radio system, meteor burst communications, and communications in regions that encompass large geographic areas, such as national forests [6]. Considering the low power transmission limit for this band, as well as the fact that it is licensed to 2-way land mobile communication [7], a primary rail application is for communication in yard operations by rail personnel, as this band supports mobile operations. Additionally, most transmissions will be in narrowband, with a channel spacing of 20 kHz. This band may also be assigned for the operation of Location and Monitoring Service (LMS) systems. Finally, in some regions this band may also be used for TV broadcasts and is known as the "I band," with a lower starting frequency at 44 MHz [8].

3.2.2 Band: 72-76 MHz

The rail industry uses this band, with a starting frequency range of 72.44 MHz and an ending frequency of 75.6 MHz, at a channelization of 40 KHz. Due to the low power limits, various mobile operations are the primary application for this band [9].

3.2.3 Band: 150-174 MHz

This band is a part of the original AAR band plan and is widely used in the United States. This band is organized into the following subgroups, based on frequency range and channel spacing [10].

- **Channels 001-097**
  This frequency range is licensed to the AAR and spans from 159.57 MHz to 161.565 MHz, with a 240 KHz channel spacing. These channels are used primarily for communication between bases and mobiles/handhelds.

  The subaudible tone, or access code, used by the output frequency is set at CarrierSquelch/No tone. The transmission mode/modulation in use for these frequencies is Frequency Modulation Narrow (FMN) with partial encryption.

- **Channels 107-196**
  The channels shown in the previous section saw an expansion when narrowbanding (i.e., the use of narrower channel spacing) was introduced by AAR. These additional channel frequencies start at 160.2225 MHz and end at 161.5575 MHz, with a narrower spacing of just 15 KHz. All other characteristics for these channels match those of the channels shown in the previous section, and these channels are also used between bases and mobiles/handhelds. These are "splinter channels" and reside in between the existing AAR channels. Interference and poor receiver design may contribute to the false detection of these channels being in use when instead it is RF leaking from the primary channels.

- **Channels 307-487**
  To enable more channels for communications, a new channelization scheme was introduced on top of the previous channels 001-097 and 107-196, but with a significantly narrower channel spacing of only 6.5 KHz. This band spans the frequency range of 160.215 MHz to 161.5725 MHz and is the primary focus of this project phase.

  These are the standard railroad digital channels used by Next Generation Digital Narrowband (NXDN) radios. However, site-specific exceptions are possible, as those radios/channels are only used at a certain terminal or function. Other characteristics of these channels remain the same as previously shown for this band.

3.2.4 Band 217-222 MHz

AAR has selected this band for operation of the PTC system across North America. This block grant scheme uses RF and GPS to control and enforce train movement regulations. PTC systems are designed to be interoperable through standardized protocols and equipment.

The frequencies allocated for PTC applications by the rail industry span from 220.1275 MHz to 220.7975 MHz, with a relatively narrow channel spacing of 5 KHz. The primary modulation scheme is Differential Quadrature Phase Shift Keying (DQPSK) for RF transmission and reception [11]. Other available modulation schemes include Binary Phase Shift Keying (BPSK)

and 8 Quadrature Amplitude Modulation (QAM), depending on prevalent RF channel conditions. A second application in this band is mobile/handheld communications, using the frequency range of 221.1275 MHz to 221.7975 MHz and adopting the FMN channel spacing and modulation scheme.

3.2.5 Band 450-470 MHz

An EOTD (End of Train Device), also known as a Flashing Rear End Device, is a fixed device installed at the end of most freight trains to monitor and report the train status to the locomotive's Head of Train Device. The train status includes train movement, brake pressure, and emergency status of the air valve along with the train-specific radio identification. The frequency of 457.9375 MHz is used for the EOTD, with Frequency Shift Keying (FSK) used as the modulation scheme for train telemetry communications [12]. The HOTD uses the 452.9375 MHz frequency with the same modulation scheme. Another application for this band is the remote control of locomotives during yard movements. The Remote-Controlled Locomotive (RCL) protocol for radios is typically found in yards and terminals. The remote train control system frequencies are 452.9 - 452.96875 MHz and 457.9 - 457.96875 MHz, with a channel spacing of 6.25 KHz. To maximize robustness, BPSK modulation is used for these types of communications [13].

3.2.6 Band 896-928 MHz

AAR has allocated this band for the radio operations of the Advanced Train Control System (ATCS), which is a wayside signaling and message delivery reporting system. There is no public plan for specific frequencies used in this band [14], but some of the reported frequencies used for ATCS are shown in Table 2. These frequencies may vary between railroad companies; examples of this are also noted in Table 2.

Table 2. Frequencies reported for use with ATCS operations

896.8875 (Union Pacific)	935.8875 (Union Pacific)
896.9375	935.9375
896.9875	935.9875
897.8875 (BNSF)	936.8875 (BNSF)
897.9375 (Norfolk Southern)	936.9375 (Norfolk Southern)
897.9875 (Southern Pacific)	936.9875 (Southern Pacific)
928.00625	928.01875
928.03125	928.04375
928.05625	928.06875

The rail industry is also using this band for the Automatic Equipment Identification (AEI) tag system, which is an RF Identification (RFID) system operating at two specific frequencies: 915 and 928 MHz. FSK modulation is used in this case due to its high resistance to noise. This band

also spans the license-free Industrial, Scientific, Medical (ISM) segment of 902928 MHz already in use for a variety of applications in the rail industry.

3.3 Band Summary

Table 3 provides a summary of the different RF bands used by the rail industry. Abbreviations used in this table are defined in Table 4. Maximum ERP is based on information from [15, 16], based on the HAAT factor.

Table 3. Rail industry RF band summary

Band (MHz)	30-50	72-76	150-174	217-222	450-470	896-928
Application	MS/LMS	MS	MS/BS	MS/PTC	TT/RCL	ATCS
Max ERP (Watts)	2-300	2-300	2-500	2-500	2-500	10-500
Frequency Range (MHz)	-	72.44-75.6	159.57-161.5725	220.1275-221.7975	452.9-457.96875	-
Channel Spacing (kHz)	20	40	240/15/6.5	5	6.25	-
Modulation	FM	FM	FMN/NXDN	DQPSK-FMN	FSK-BPSK	-
Information Type	Voice & Data	Voice	Voice & Data	Voice & Data	Data	Data

Table 4. Application abbreviations shown in Table 3

Application Abbreviation	Definition
MS	Mobile
LMS	Location and Monitoring Service
BS	Base station
PTC	Positive Train Control
TT	Train Telemetry
RCL	Remote Controlled Locomotives
ATCS	Advanced Train Control System

4. Simulation of RF Propagation Characteristics

To analyze the communication performance of the available RF bands, the team worked to identify a suitable simulation platform for analysis. Simulation platforms can generally be grouped into electromagnetic (EM) field simulation solutions, networking simulation solutions, and channel modeling and propagation simulation solutions. Available simulation platforms within each category were investigated to identify the most suitable candidate for this research phase.

4.1 EM Simulation Platforms

A comprehensive literature survey was performed to identify and evaluate various EM simulation platforms. Below is a list of the most prominent and widely used solutions in this category.

- Numerical Electromagnetics Code (NEC) [17]: NEC is an open-source platform that can be installed on both Windows and Linux operating systems and is equipped with intuitive analysis via 3D modeling and visual representation. This platform uses the Method of Moments (MoM) computational method to solve the linear partial differential equations and obtain parameters of the modeled EM field with a manual mesher. However, this platform is typically used for antenna modeling, and is widely used as the basis for many Graphical User Interface (GUI)-based programs on many platforms (e.g., popular distributions such as 4nec2 and EZnec on Windows, xnec2c on Linux, and cocoaNEC for Mac OS X). Version 2 is open source, but Versions 3 and 4 are commercially licensed.
- Momentum [18]: Momentum is a commercial platform that can be run on both Windows and Linux operating systems. It is equipped with partial 3D visualization through its GUI interface and uses the same MoM algorithm as NEC, with an equidistant method for meshing. Moreover, it can automatically control results convergence. Its applications are primarily found in passive planar elements development, integrated into the Agilent EEsof Advanced Design System.
- HFSS [19]: HFSS is a commercial platform capable of being installed on both Windows and Linux operating systems and fully supports 3D and GUI interfacing. Compared to other simulation platforms, HFSS supports many different numerical solvers for the partial differential EM field equations, including the Finite Element Method (FEM), Finite-Difference Time-Domain (FDTD), Hybrid Finite Element - Boundary Integral [20], MoM, and Eigen mode. To provide a more automatic process for this platform, the mesher is designed to be adaptive based on the desired simulation. Its broad applications include the analysis of antenna/filter/IC packages, Radome designs, RFIC, Low-Temperature Co-fired Ceramics (LTCC), Monolithic Microwave Integrated Circuit, antenna placement, wave guides, Electromagnetic Interference (EMI), Frequency Structure Simulation (FSS), metamaterial research, composite materials, Rich Communication Services-Mono and Bi development.
- XFdtd [21]: The XFdtd commercial platform is also capable of being installed on both Windows and Linux while supporting 3D and GUI interfacing, but it uses only the FDTD algorithm for obtaining results. Its mesher method is automatically optimized based on the project for user convenience. XFdtd applications encompass RF and microwave antennas,

components, and systems such as mobile devices, Magnetic Resonance Imaging (MRI) coils, radar, wave guides, and Synthetic-Aperture Radar (SAR) validation.

- AWR Axiem [22]: AWR Axiem is a commercial platform that provides many of the same features as the previous solutions but is built around a different solver, mesher method, and application domain. Its solver uses the MoM approach coupled with a mesher that supports automatic and hybrid methods. Its applications include Printed Circuit Board (PCB) analysis (e.g., multi-layer PCBs, LTCC, High-Temperature Co-fired Ceramics, on-chip passives, and printed antennas). It is primarily focused on planar structures and is also integrated into Microwave Office.
- AWR Analysis [22]: This commercial platform is similar to AWR Axiem but also supports 3D structures. It uses FEM as the solver, instead of MoM, which enables it to include all applications supported by AWR Axiem as well as other applications, such as 3D Antennas, wave guides, 3D filters, and more complex PCBs. It is also integrated into Microwave Office.
- JCMsuite [23]: This commercial platform is very similar to AWR Analysis but uses a different mesher that incorporates methods for automatic error control. This makes this platform suitable for analysis of nano- and micro-photonic applications (e.g., light scattering, wave guide modes and optical resonances).
- COMSOL Multiphysics [24]: This general-purpose commercial platform differentiates itself from its competitors through its use of FEM, a boundary element method, ray tracing as its solver, and it supports a fully automatic mesher.
- FEKO [25]: This commercial platform uses MoM, FEM, FDTD, a Fast Multipole Method, physical optics, geometrical optics or ray optics, as well as the uniform geometrical theory of diffraction as solver algorithms. Its mesher method can operate in manual mode or as a fully automatic mesher that adapts to the project requirements. Its applications include antenna analysis, antenna placement, windscreen antennas, microstrip circuits, wave guide structures, radomes, EMI, cable coupling, FSS, metamaterials, periodic structure, and RFID.
- Elmer FEM [26]: This open-source platform uses only FEM for its solver, and its mesher can operate manually or use imported meshes. It is used for the general-purpose analysis of 2D and 3D magnetics, both static and harmonic. Its 3D solver is based on the Whitney AV formulation of Maxwell's equations.

4.2 Networking Simulation Platforms

The team identified the following network simulator platforms available for this project phase.

- Cisco Packet Tracer [27]: Packet Tracer is Cisco's visual simulation tool. It simulates network topologies comprised of Cisco routers, switches, firewalls, and more. Packet Tracer has several benefits (e.g., a free network simulator, including its cost, cross-platform compatibility, device variety, and connection variety) making it suitable for the analysis of different network topologies. However, it is limited in RF analysis.
- OMNet++ [28, 29]: OMNeT++ is a discrete-event simulator for modeling communication networks, multiprocessors, and other distributed or parallel systems.

OMNeT++ is open-source and can be used under an academic public license that makes the software free for non-profit use. OMNeT++ was developed to produce a powerful open-source, discrete-event simulation tool that can be used by academic, educational, and research-oriented commercial institutions for the simulation of computer networks and distributed or parallel systems. OMNeT++ attempts to fill the gap between open-source, research-oriented simulation software like NS2 and expensive commercial alternatives like OPNET.

- Boson NetSim [30]: Boson NetSim is an application that simulates Cisco network routers and switches. It supports the customization of the available models and a wide array of different simulation scenarios. However, like the Cisco Packet Tracer it is less suitable for RF analysis.
- Graphical Network Simulator 3 (GNS3) [31]: GNS3 is a free, open-source client/server interface for network emulation and virtualization. It is a Python-based platform that primarily uses software called Dynamips to emulate Cisco software and hardware. Since Dynamips supports the Cisco 1700, 2600, 2691, 3600, 3725, 3745, and 7200 router platforms, GNS3 also supports these platforms. In recent years, however, GNS3 has evolved to support a larger scope of virtual network devices from a variety of vendors using "appliances," which are easy-to-import templates of common virtual network devices. Its benefits can be generally categorized as being free/open-source, simple to use, and supporting modifiable active topology and multiple connection types.
- Virtual Internet Routing Lab (VIRL) [32]: VIRL is Cisco's proprietary virtual network emulator designed for educational institutions and individuals. It is very similar to Cisco Modeling Labs, which is a highly scalable variant of VIRL designed for medium and large businesses to model and emulate enterprise networks. VIRL operates in a client/server model like GNS3. This network emulator has the advantages of network topology portability and advanced automation capabilities.
- Emulated Virtual Environment Next Generation (EVE-NG) [33]: EVE-NG is a multi-vendor virtual network simulator that was developed for individuals and smaller businesses. It has both a free and licensed version available. Some of its advantages are itsIt is advantageous because it is low cost, clientless, uses a modifiable active topology, and has multiple connection types.
- OPNET [34]: OPNET is a tool to simulate the behavior and performance of any type of network. The main differentiator between OPNET and other simulators is its power and versatility. It provides pre-built models of protocols and devices and allows the user to create and simulate different network topologies. Some of its provided protocols/devices are expandable. OPNET provides both a commercial and free license.

Following is a list of commercial and open-source network simulators and network emulators that run on the Linux or BSD operating systems [35] in addition to Windows.

- Network Simulator 3 (NS3) & NS2 [36]: NS3 is a discrete-event, open-source network simulator for internet systems used primarily for research and educational use. NS3 is a complex tool that runs simulations described by code created by users. Therefore, a substantial level of expertise in programming is required to use this simulator. NS3 can run real software on simulated nodes using its direct code execution feature, which allows

researchers to test real software or web servers in a discrete-event network simulation environment to produce repeatable experiments. NS3 is intended to replace NS2, which is the previous major version of this network simulator; NS2 is no longer maintained but is still widely used by researchers.

- Antidote (NRE Labs) [37]: Antidote is a network emulator combined with a presentation framework designed to create and deliver networking technology training. Its user interface operates in a web browser, including the terminals that the user can access to run commands on emulated network devices and servers.
- Cloonix [38]: The Cloonix network simulator provides a relatively easy-to-use graphical user interface. Cloonix uses QEMU/KVM emulators to create virtual machines. Cloonix provides a wide variety of pre-built file systems that can be used as virtual machines and provides simple instructions for creating other virtual machine root file systems. Cloonix has an active development team updating and improving the tool every two to three months.
- Common Open Research Emulator (CORE) [39]: CORE provides a GUI interface and uses the network namespaces functionality in Linux containers as a virtualization technology that allows CORE to start up a large number of virtual machines quickly. CORE supports the simulation of fixed and mobile networks and can run on both Linux and FreeBSD. CORE is a branch of the IMUNES network simulator and expands on its functionality in myriad ways.
- Integrated Multi-Protocol Network Emulator/Simulator (IMUNES) [40]: IMUNES was developed at the University of Zagreb for use as a network research tool and runs on both the FreeBSD and Linux operating systems. It uses the kernel-level network stack virtualization technology provided by FreeBSDand uses Docker containers and Open vSwitch on Linux. IMUNES supports a GUI and provides excellent performance even when running in a virtual machine.
- Mininet [41]: Mininet is designed to support research in software defined networking (SDN) technologies. It uses Linux network namespaces as its virtualization technology to create virtual nodes. and is designed to support thousands of virtual nodes on a single operating system. Mininet is most useful to researchers looking to verify the behavior and performance of SDN controllers. Knowledge of the Python language is required when using Mininet, although excellent user documentation is provided. Researchers have created branches of Mininet that focus on specific technologies such as Mini-NDN, Mini-CCNx, Mininet-WiFi, and ESCAPE protocols.
- Shadow [42]: Shadow is an open-source network simulator/emulator hybrid that runs real applications like Tor and Bitcoin over a simulated internet topology on a single Linux computer. Users run a simulation by creating an eXtensible Markup Language (XML) file to describe the network topology and plugins to link their application code to nodes in the simulation. Shadow operates as a discrete-event simulator so that experiments are repeatable. Shadow can also run real software on its virtual nodes while using plugins created by the user. This combination of features makes Shadow a unique tool for network simulations.

- Virtual Networks over Linux (VNX) and Virtual Network User Mode Linux (VNUML) [43]: VNX supports two different virtualization techniques and uses an XML-style scripting language to define the virtual network. It also supports chaining multiple physical workstations together to support distributed virtual labs that operate across multiple physical workstations. VNX is the successor to VNUML.

4.3 Channel Modeling or Environment Propagation Simulation Platforms

Environment propagation simulation platforms have been specifically designed to analyze various propagation parameters and models under certain conditions, such as 5G wireless communications that involve millimeter waves. Following are some of the most prominent channel modeling simulation platforms.

- Volcano 5G [44]: Volcano 5G is an innovative propagation model to design any wireless network, including 5G and IoT networks in any environment, including millimeter wave applications. Some of its advantages are accuracy, fast modeling, model calibration, and algorithm optimization.
- S-5GChannel [45]: S-5GChannel is a comprehensive simulation tool for 3D channel modeling combining the Volcano model suite, accurate 3D visualization, analysis capabilities, and 3D Geographic Information System data to simulate and analyze propagation in any frequency band and any outdoor or indoor environment.
- MATLAB [46]: MATLAB, including its communications toolbox, provides algorithms and applications for the analysis, design, end-to-end simulation, and verification of communications systems. This solution's algorithms include channel coding, modulation, Multiple-Input Multiple-Output, and Orthogonal Frequency-Division Multiplexing. MATLAB enables the user to compose and simulate a physical layer model of a standard-based or custom-designed wireless communications system.

5. Single-Carrier Modulation Study

Based on the research gathered in Section 4, and considering available resources, expertise from past efforts, and project time constraints, MATLAB was selected as the primary simulation environment for this project. It was chosen for its physical layer considerations (e.g., modulation, propagation, error correction coding) and the protocol simulation shown in later sections.

Once MATLAB was selected, the team built a framework to evaluate a wide range of modern modulation schemes. Table 5 shows the modulation schemes and the respective modulation orders evaluated.

Table 5. Investigated modulation schemes and their order

Modulation Scheme	Modulation Order
QAM	2 – 4 – 8 – 16 – 32 – 64 – 128 – 256
Mil88QAM	16 – 32 – 64 – 256
Amplitude and phase-shift keying (APSK)	16 – 32 – 64
Digital Video Broadcasting (DVB)-S2-APSK	16 – 32
DVB-S2X-APSK	16 – 32 – 64 – 128 – 256
DVB-SH-APSK	16
PSK	16 – 32 – 64 – 128 – 256
Pulse-Amplitude Modulation (PAM)	16 – 32 – 64 – 128 – 256

For each modulation scheme and its orders, the team evaluated the maximum bitrate supported by the scheme as well as the required Root Raised Cosine transmit filter parameters (these parameters allow the transmitter to satisfy the FCC-mandated spectral mask for the channel scheme on the 160 MHz band). Both 6.25 kHz and 12.5 kHz channelization were evaluated and a 1W transmit power setting was used. Figure 2 shows the spectrum analyzer view of a 6.25 kHz channel scheme with its spectral mask, plus the spectrum plot of a 64-QAM scheme at 30 kbps.

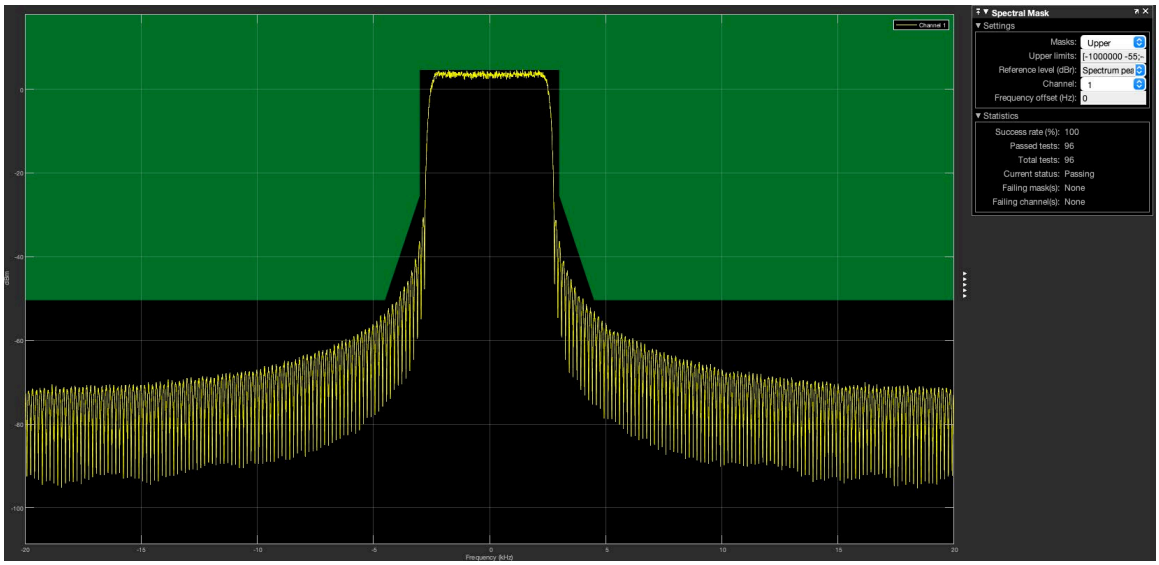

Figure 2. Spectrum view of a 64-QAM signal and a 6.25 kHz channel

A total of 66 channel+modulation configurations were tested and the team compiled results for achievable symbol rate, maximum bit rate, and transmit pulse shaping filter configurations that satisfy spectral mask requirements. All configurations were tested for a 1W reference power. In future test configurations, the transmit power will be varied to be representative of the currently prevalent transceiver designs for 160 MHz applications (e.g., NXDN radios).

The following graphs show the results for achievable symbol rate and bit rate. Commonplace modulation schemes (e.g., QAM) were tested, as well as less common candidates (e.g., Mil88 and DVB-S2X).

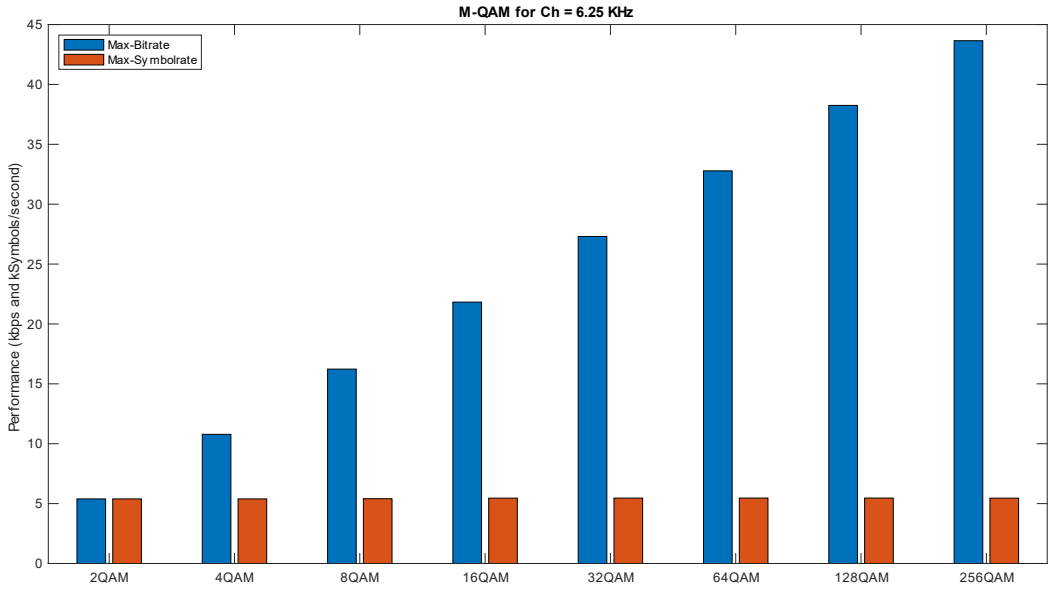

Figure 3. Results for QAM with different modulation orders at a 6.25 kHz channel width

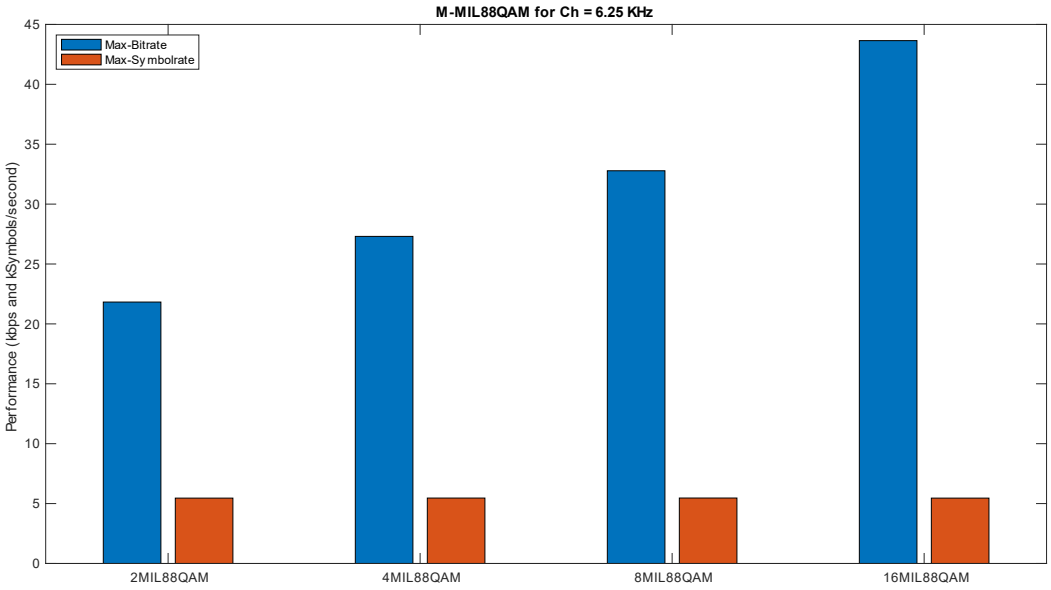

Figure 4. Results for Mil88 with different modulation orders at a 6.25 kHz channel width

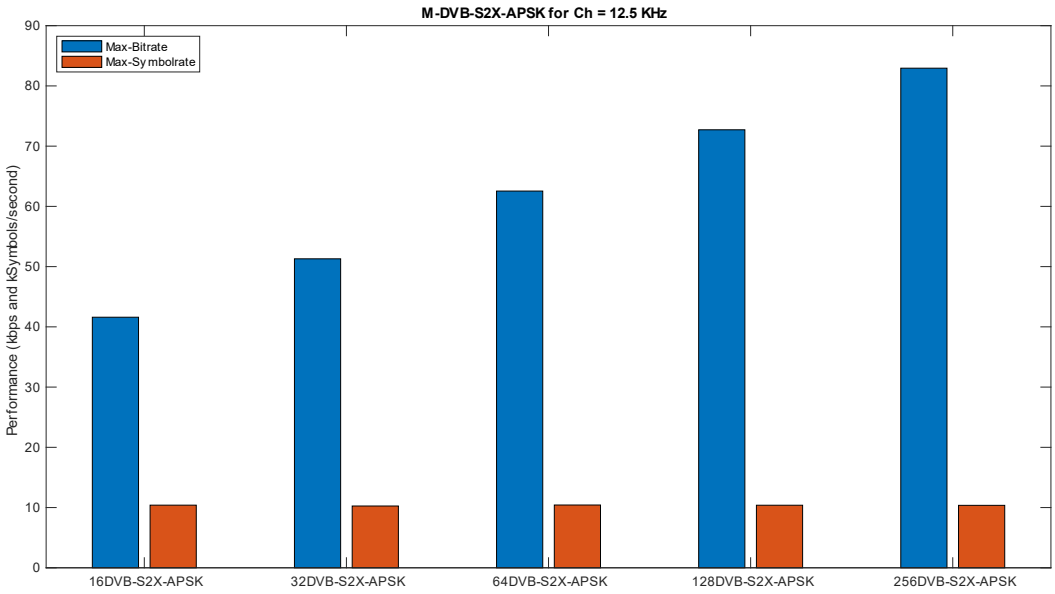

Figure 5. Results for DVB-S2X with different modulation orders at a 12.5 kHz channel width

All the schemes evaluated previously are single-carrier schemes, such as QAM, APSK, or DVB. Single-carrier schemes are ideally suited for scenarios where endpoint links were used (e.g., point-to-point connections). Point-to-multipoint schemes, such as multiple mobile devices associated with a single base station, require methods for multiplexing their data together to control modulation and coding and compensate for varying distances between individual mobiles and the base station, as well as methods for handling resource allocation.

6. Modulation Study of OFDM with QAM

OFDM is widely used in modern communication protocols, from 4G and 5G to DSL and beyond. OFDM splits the frequency band, or channel, into multiple subbands. Each subband is handled by a single subcarrier. The collection of subcarriers at a moment in time is called an OFDM symbol. Multiple OFDM symbols are grouped into a frame with a given duration. The advantage of OFDM is that each subcarrier can be individually modulated and use different modulation schemes. This allows allocation of some subcarriers to a distant mobile node, using BPSK as the subcarrier modulation for a more robust signal; other subcarriers in the same OFDM symbol can be modulated using another signal (e.g., 256-QAM) to provide higher performance for a much closer mobile node.

Different OFDM configurations for the 160 MHz band were evaluated for the highest possible performance. MATLAB/Simulink continued to be used for the modulation and propagation simulation framework.

The visualization in Figure 6 shows an example spectrum plot of an OFDM modulation signal that uses 32 subcarriers, with a single guard subcarrier on each side and the DC (center) subcarrier zeroed out. Each individual ripple in the center region of the plot represents a subcarrier that can individually be modulated. A total of 32 subcarriers were chosen for this example, but at 160 MHz, higher subcarrier counts have been successfully tested.

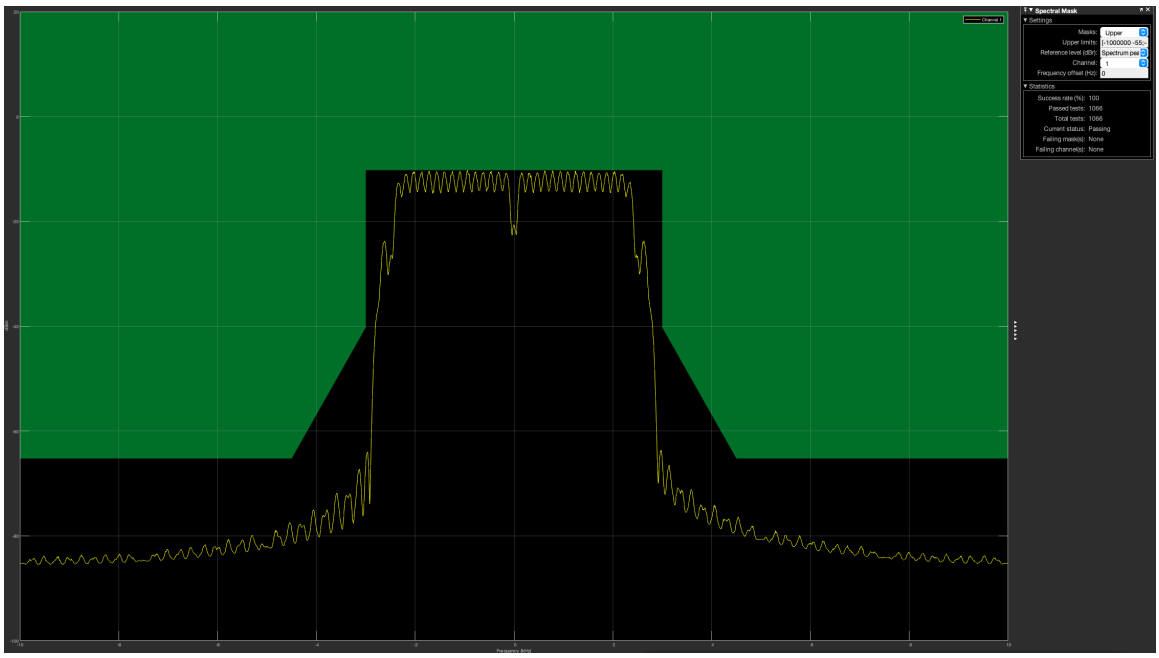

Figure 6. Spectrum plot of an OFDM signal with 32 subcarriers

OFDM was evaluated for a wide variety of permutations of all the controllable parameters. The resulting maximum performance achieved is shown in Figure 7.

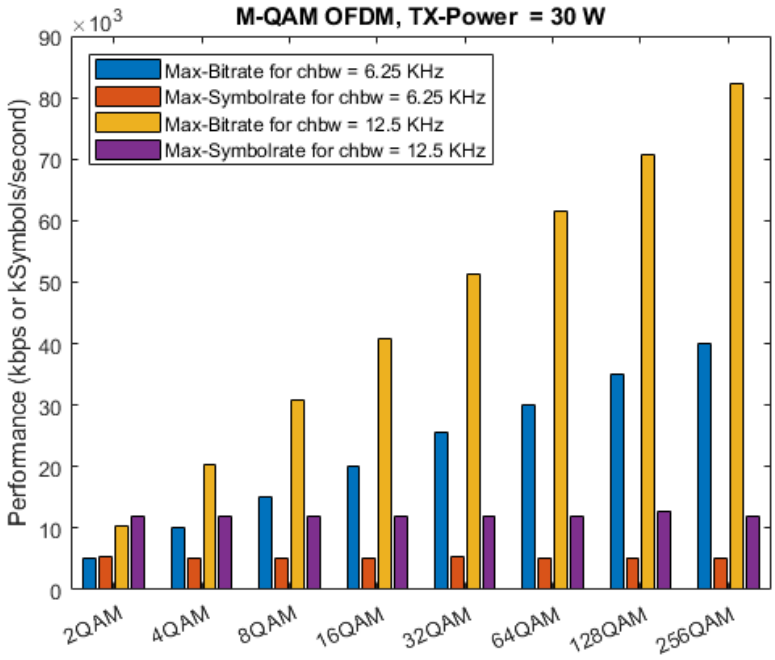

Figure 7. Maximum OFDM Performance Results

In this test, all usable data subcarriers (excluding guard bands and the DC subcarrier) were modulated using the same QAM modulation scheme and order. A reference power of 30 W was used for the transmitter, for spectral mask considerations.

For 6.25 kHz channels, the maximum transmit data rate is approximately 40.02 kbps, and for 12.5 kHz channels it is approximately 82.18 kbps.

For 6.25 kHz, the highest-performant configuration is shown in Table 6.

Table 6. Configuration for 6.25 kHz channels with OFDM

FFT Size	256
Cyclic Prefix Size	8
Guard Subcarriers + DC Subcarrier	2
Windowing	Yes
Subcarrier Modulation and Order	256-QAM
Sample Rate	5200 samples per second
OFDM Symbol Rate	19.697 symbols per second
Data Subcarriers per OFDM Symbol	254

Similarly, for 12.5 kHz, the highest-performance configuration is shown in Table 7.

Table 7. Configuration for 12.5 kHz channels with OFDM

FFT Size	256
Cyclic Prefix Size	8
Guard Subcarriers + DC Subcarrier	30
Windowing	Yes
Subcarrier Modulation and Order	256-QAM
Sample Rate	12000 samples per second
OFDM Symbol Rate	45.45 symbols per second
Data Subcarriers per OFDM Symbol	226

7. Coding Scheme Evaluation

Error correction coding, also known as Forward Error Correction (FEC), is a technique commonly deployed in wireless communication schemes where noisy environments result in bit errors within the received data stream. Combined with the adaptive selection of a modulation scheme, this Modulation and Coding Scheme (MCS) provides a highly effective mechanism to adapt the communication for a wireless link to the prevalent channel conditions. When those conditions change (e.g., in mobile environments), the adaptive selection of suitable MCS schemes occurs. This is also often referred to as Adaptive Modulation and Coding (AMC).

A variety of different coding schemes have been developed. They provide a balance between the computation complexity of their implementation and the effective reduction in bit errors they can achieve.

These coding schemes work by leveraging redundant information being transmitted between transmitter and receiver. The receiver can use this redundant information to effectively detect and repair bit errors. However, its inclusion means that the available effective bit rate is reduced to accommodate the redundant information within a given channel.

Table 8 summarizes the reviewed coding schemes.

Table 8. Overview of different Error Correction Coding schemes

Coding Schemes	Decoding Complexity (Required Time)	Typical Code rate	Operation Scheme	Features
AN Code [47]	-	-	-	-
BCH Code [48]	$O(\delta n log n)$ n: codeword length delta: distance	-	Block (Galois Field)	• Precise control over the number of symbol errors correctable by the code • Easy algorithm for decoding (syndrome decoding)
Berger Code [49]	No decoding (Detection-based)	-	-	• Detect any number of one-to-zero bit-flip errors, if no zero-to-one bit-flip errors occur • Detect any number of zero-to-one bit-flip errors, if no one-to-zero bit-flip errors occur
Constant-weight code (m-of-n code) [50]	$O(w^2)$ W: codeword weight	-	Block	• Can operate like Berger codes
Convolutional Codes [51]	$O(n2^K)$ – soft decision n: message length K: Constraint length	1/2 – 2/3 – 3/4 – 5/6 – 7/8	Stream	• Ability to perform economical maximum likelihood soft decision decoding • More efficient than other encoding schemes except turbo codes
Expander Codes [52]	$O(n)$ n: block length		Block	• No large alphabet size like Reed-Solomon codes

Coding Schemes	Decoding Complexity (Required Time)	Typical Code rate	Operation Scheme	Features
Binary Golay Codes [53]	$O(n)$ n: block length		Block	• G24 (a sub-category of BGC codes) can correct any 3 bits in error or detect any 7 bits in error
Goppa Codes [54]	-	-	-	-
Hadamard Codes (Walsh Codes) [55]	$O(n \log n)$ n: block length	k/2^k k: message length	Block	• Used for error detection and correction when transmitting messages over very noisy or unreliable channels
Hamming Codes [56]	$O(n^2)$ $2^n - 1$: block length	1-n/$2^n - 1$	Block	• Can detect up to two-bit errors or correct one-bit errors without detection of uncorrected errors → limited practical scale • Bandwidth usage is more → reduces the effective bitrate in transmission
Latin Square Codes [57]	-	-	-	-
Long Codes [58]	-	-	Block	• Extremely poor rate
LDPC (Gallager) Codes [59]	$O(n^2)$ n: block length (data bits) Reduced Version $O(n)$ n: block length	3/4 – 5/6 – 7/8	Block	• Allows the noise threshold to be set very close to the theoretical maximum (the Shannon limit) for a symmetric memoryless channel • Has no minimum distance limitations, which indirectly means that LDPC codes may be more efficient on relatively large code rates (e.g., 3/4, 5/6, 7/8) than Turbo codes • Has a better block error performance and a better performance on bursty channels compared to turbo codes • Is more amenable to high rates, and can be designed for almost any rate and block-length (in contrast, the rate of turbo codes is usually adjusted by a puncturing scheme, which requires an additional design step) • LDPC error floor tends to occur at a lower BER compared to turbo codes • A single LDPC code can be universally good for a collection of channels

Coding Schemes	Decoding Complexity (Required Time)	Typical Code rate	Operation Scheme	Features
Turbo Codes [60]	$O(n)$ n: block length	1/2 – 1/3 – 1/4 – 1/6 –3/4 – 4/5 – 6/7	Block	• Turbo codes are the best solution at the lower code rates (e.g., 1/6, 1/3, 1/2) • First practical codes to closely approach the maximum channel capacity or Shannon limit • Achieve reliable information transfer over bandwidth- or latency-constrained communication links in the presence of data-corrupting noise • Similar performance with LDPC codes
Reed-Solomon Codes [61]	$O(n^2)$ n: code length	RS(255,251) RS(255,239) RS(255,223)	Block	• Able to detect and correct multiple symbol error • Optimal in the sense that the minimum distance has the maximum value possible for a linear code
Reed-Muller Codes [62]	RM(m,r) n = $2^{m+1}/2$ ML decoder: $O(n^2)$ Fast Hadamard Transform decoder: $O(n\ log\ n)$	Rate = k/2^m k: message length 2^m: Block length RM(1,3) - RM(2,3) RM(2,5) – RM(2,4) RM(3,4) – RM(4,5)	Block	• Reed–Muller codes generalize the Reed–Solomon codes and the Walsh–Hadamard code
Polar Codes [63]	$O(n\ log\ n)$ n: block length	1/2 – 1/3 – 2/3 – 2/4 – 3/5 – 5/6	Block	• In block sizes that industry applications are operating, the performance of the successive cancellation is poor compared to well-defined and implemented coding schemes (e.g., LDPC and Turbo codes)

All these codes are governed by a code rate, which indicates the ratio of original data bits to total resulting coded bits. For example, a code rate of 2/3 indicates that within a transmitted block of 3 bits, 2 bits are original data and 1 bit is redundancy information. Hence, 1/3 of the total bit rate is used for redundancy information.

When using MCS schemes, the usable data rate can easily be calculated as

$$BR_{usable}=BR_{total}\ R_c,$$

where BR_{usable} is the usable bitrate, BR_{total} is the total bit rate, and R_c is the code rate.

8. Path Loss Estimation evaluation

The team identified and evaluated suitable path loss estimation models. To determine the performance of a transceiver design – the transmitter and receiver pair – researchers considered the RF channel conditions which dictate the quality of the received signal, typically expressed as a signal to noise ratio (SNR). The lower the SNR the higher the bit error rate (BER) at the receiver when decoding and demodulating a received signal. The difference in signal strength between the transmitter and the receiver is commonly referred to as Path Loss (PL). The path loss is governed by the actual environment and is virtually impossible to determine precisely, since it is influenced by a vast number of uneasily quantifiable parameters like air humidity, solar activity, movement of objects (signal scatterers) within an environment, and surface properties of any objects in the environment. For this reason, the channel is represented by an approximation model. These path loss models are typically applicable for different specific environments, such as rural versus urban environments, different multipath representations, etc. The choice of path loss model directly impacts the predicted distance and performance of a transceiver configuration.

For this study, a variety of different channel models were evaluated and their predicted path loss versus distance profiles were calculated to select the most suitable model for different targeted environments.

Figure 8 shows a subset of the different models evaluated, specifically for 160 MHz, including the calculated received signal power, given a transmit power of 30 W and the predicted path loss for each model.

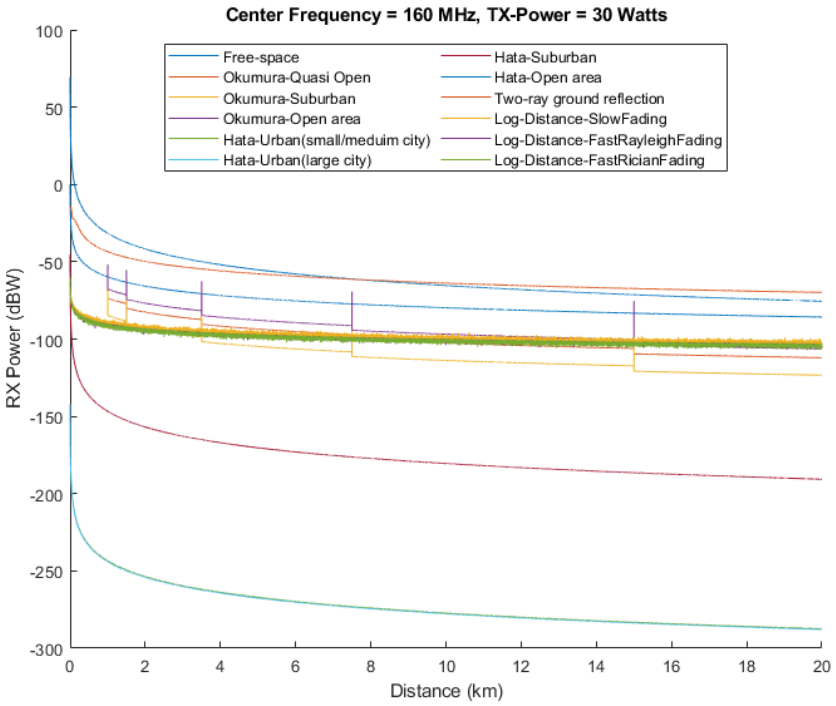

Figure 8. Path loss models and their predicted RX power

The Winner2 model was found to excel at representing different environment scenarios with high accuracy. This model is defined and characterized for the RF spectrum of 2 GHz-6 GHz,

which is outside the 160 MHz frequency range and therefore technically not applicable to this study. However, the team evaluated the predicted path loss at 160 MHz to determine if this model could actually be used. Figure 9 shows different scenarios evaluated with Winner2 at 160 MHz.

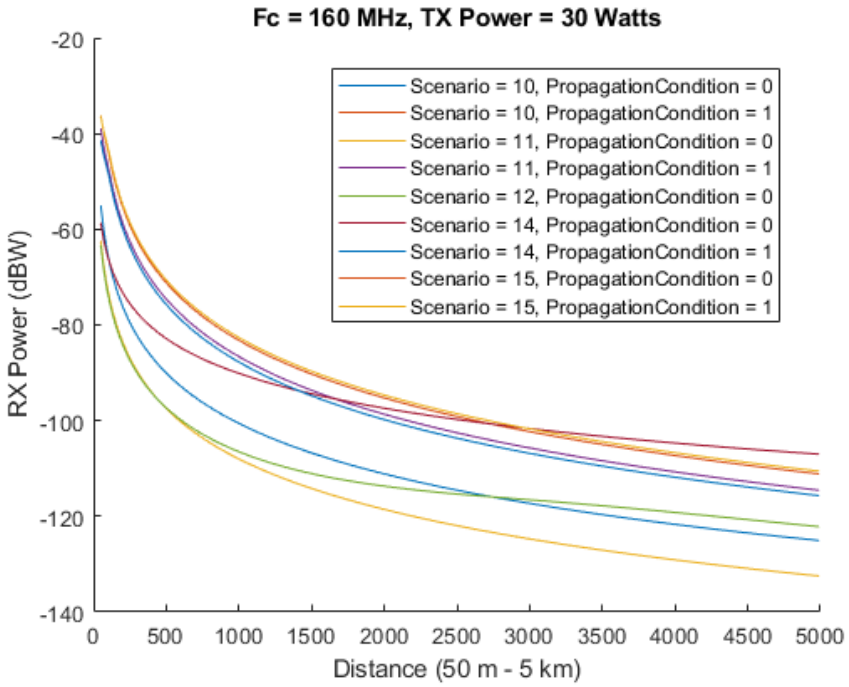

Figure 9. Winner2 path loss model and its predicted RX power

In this figure, the scenario number represents different preconfigured scenarios available within Winner2. The table below lists those scenarios supported by MATLAB's Winner2 implementation. A full list of scenarios is available from Information Technology Society [64]. The PropagationCondition parameter indicates if the Line of Sight (LOS) path was available (PropagationCondition=1).

Table 9. Winner2 scenarios supported by MATLAB

Scenario #	Winner-2 Scenario Designation	Winner-2 Scenario Name	LOS / NLOS
1	A1	Indoor Office / Residential	LOS + NLOS
2	A2	Indoor to Outdoor	NLOS
3	B1	Urban Microcell	LOS + NLOS
4	B2	Bad Urban Microcell	NLOS
5	B3	Large Indoor Hall	LOS + NLOS
6	B4	Outdoor to Indoor Microcell	NLOS
10	C1	Metropolitan Suburban	LOS + NLOS
11	C2	Metropolitan Urban Macrocell	LOS + NLOS
12	C3	Metropolitan Bad Urban Macrocell	NLOS
13	C4	Outdoor to Indoor Macrocell	NLOS
14	D1	Rural Macrocell	LOS + NLOS
15	D2a	Rural Moving Mobile Node	LOS

Although there was some correlation between the Winner2 results and the other evaluated models, the team could not conclude from the data that the predicted path loss was accurately representing the target environment. Therefore, Winner2 was of limited use within the study.

Finally, a MIMO scattering channel model available in MATLAB was evaluated, which may be of use particularly if the transceiver design incorporates Spatial Diversity (SD) MIMO. A 2x2 MIMO configuration in a path loss study was used for this evaluation and the results are shown in Figure 10.

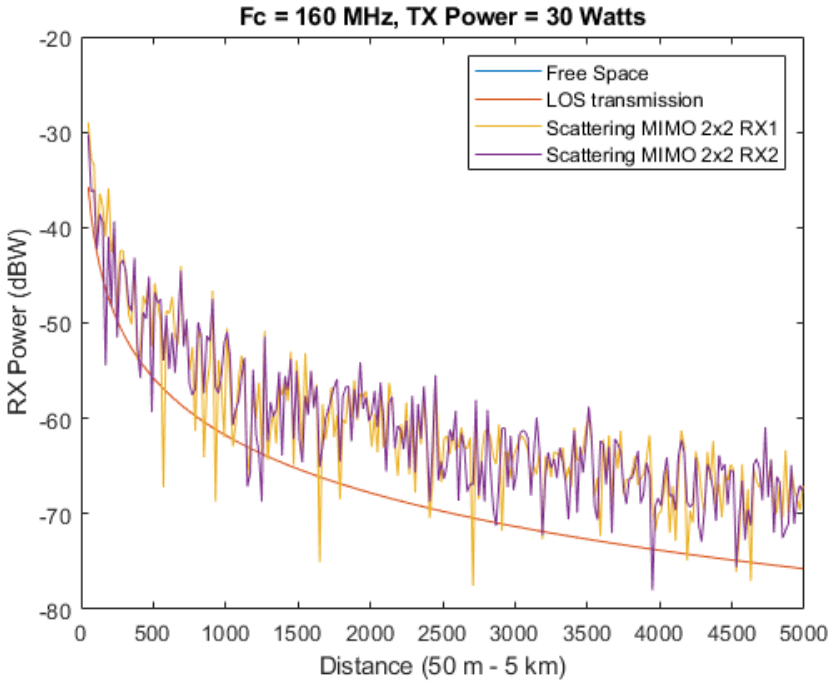

Figure 10. Scattering path loss model results

The Free Space Path Loss (FSPL) model and MATLAB's LOS-only path loss model were also plotted for comparison; the two match precisely and thus appear plotted on top of each other.

The large variability in the two scattering plots shows the impact of multipath transmissions, where the signal is scattered by objects within the environment and the resulting received signal is the combination of LOS and non-LOS (NLOS) signal paths. These paths sometimes combine destructively or constructively, which results in what is commonly referred to as Multipath Fading.

The results obtained from the modulation and coding scheme analysis, plus the results from the path loss model study, provided the necessary data to conduct and complete transceiver design.

9. Transceiver Design

The transceiver design was influenced by the theoretical study results presented in the previous sections for a 160 MHz wireless radio architecture. The first phase in this effort was to investigate a single-carrier solution using various QAM modulation schemes. Forward Error Correction techniques were then incorporated into this architecture and an OFDM-based architecture was also investigated.

9.1 Single Carrier Transceiver Without Error Correction Coding

The single-carrier effort is a vital step in ensuring a gradual adoption and evaluation of techniques for timing recovery, phase recovery, and frequency recovery on the receiver side – all important aspects in designing a robust, high-performant transceiver architecture suitable for a variety of RF environments.

The high-level block design of the initial single-carrier transceiver architecture is shown in Figure 11.

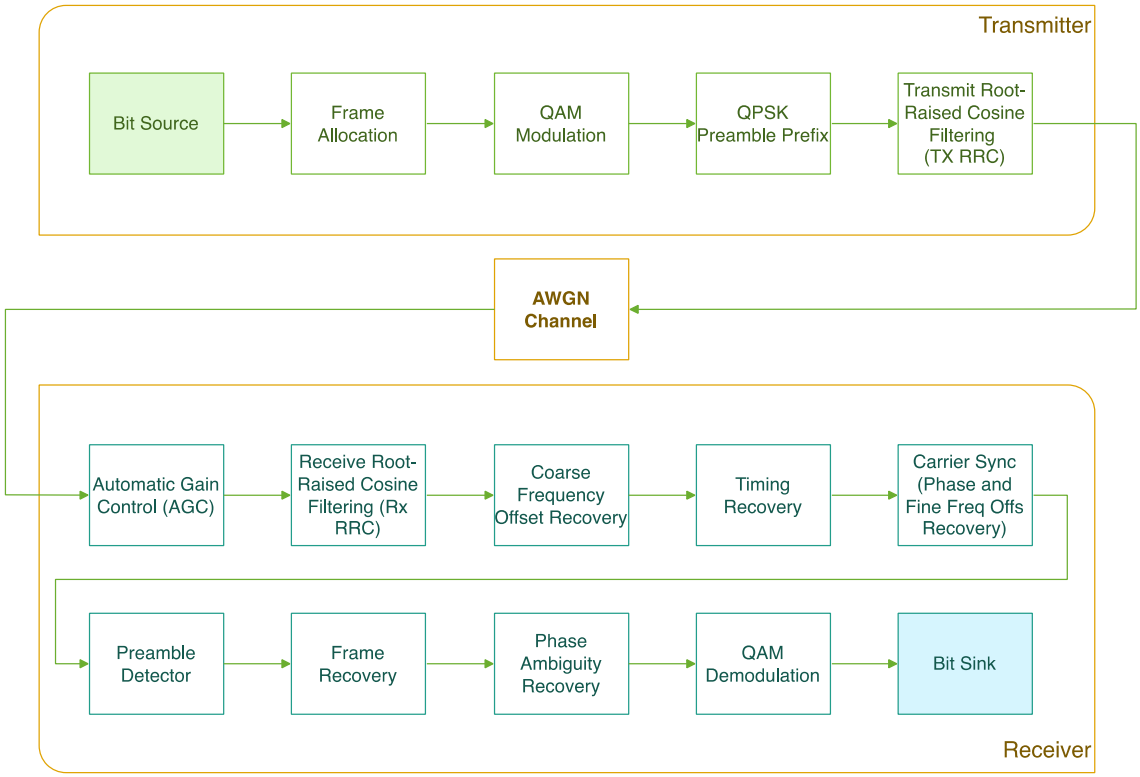

Figure 11. Initial single-carrier transceiver design without error correction coding

All the functionality was implemented in MATLAB and a full transmitter -> channel -> receiver processing flow was simulated. Several of the propagation models presented in earlier chapters were selected for the channel to obtain insights into how this transceiver will perform under a variety of different channel conditions. Most importantly, the achievable throughput at various transmitter-receiver distances was evaluated. The graphs in Figure 12 through Figure 16 show some of the results.

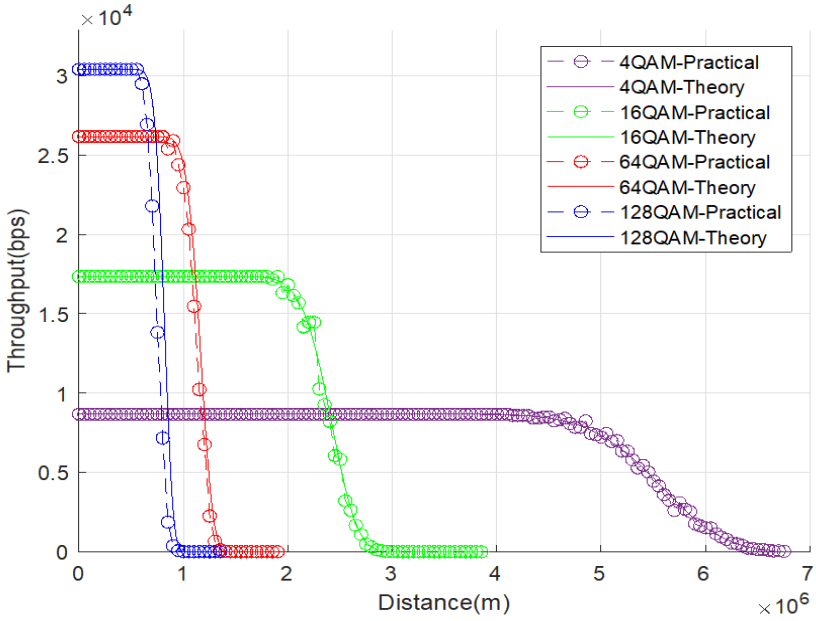

Figure 12. Single-carrier throughput versus distance for free space path loss

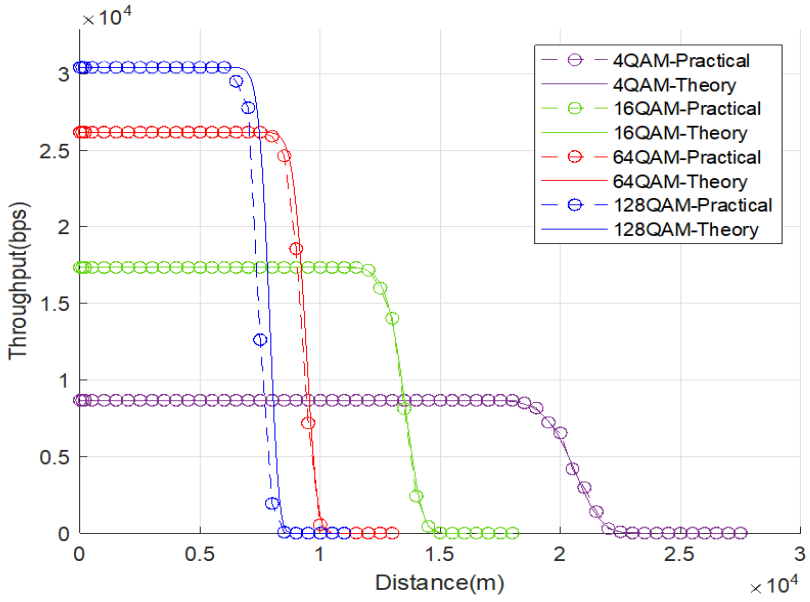

Figure 13. Single-carrier throughput versus distance for the two-ray ground model

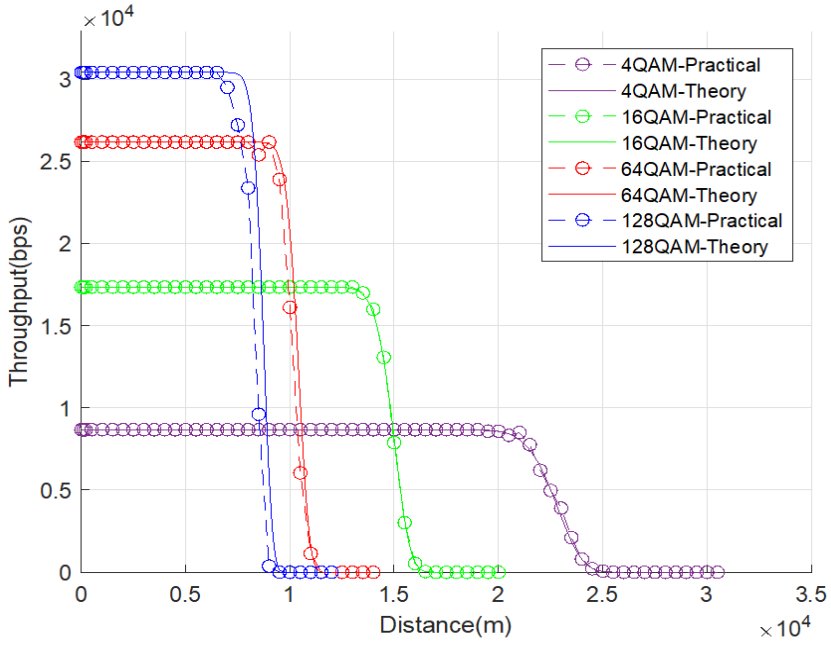

Figure 14. Single-carrier throughput versus distance for Winner2 D1-LOS (open rural environment) model

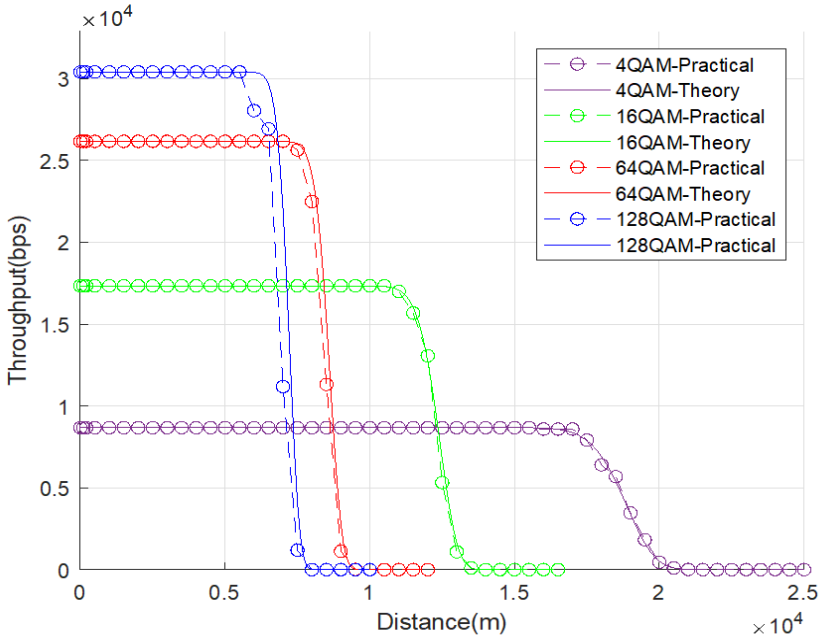

Figure 15. Single-carrier throughput versus distance for Winner2 C1-LOS (suburban environment) model

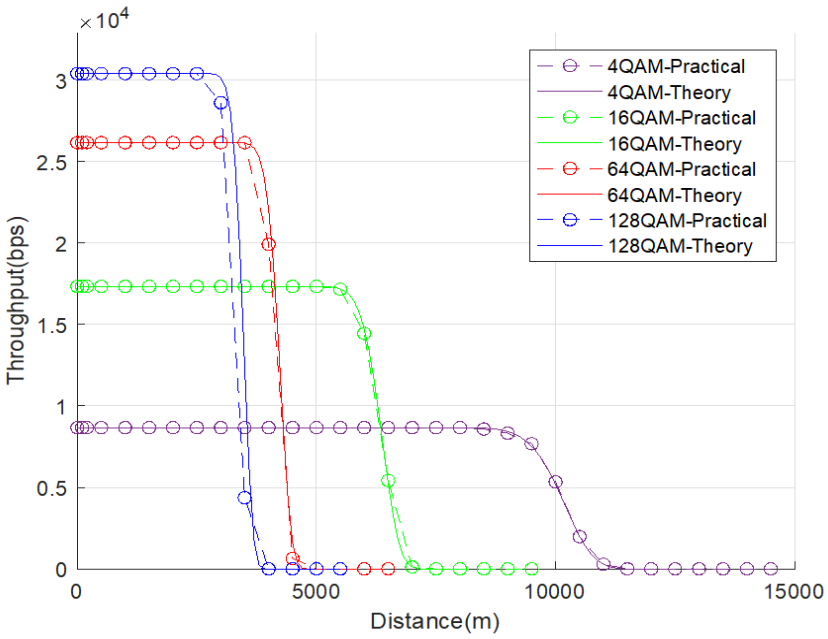

Figure 16. Single-carrier throughput versus distance for Winner2 C2-NLOS (dense urban environment) model

All results are obtained for a 6.25 kHz channel using 1 W reference power. The simulation results closely matched the expected theoretical results which validates the simulation model.

Due to the low RF frequency of 160 MHz, the resulting overall path loss was very low, which results in large, predicted communication distances. These results validate using 160 MHz RF for long-range, low-latency communications.

However, these results do not consider a radio horizon as a distance limiter. Therefore, real-world results would differ from these theoretically predicted results based solely on path loss estimations through the channel models.

9.2 OFDM Transceiver Design without Error Correction Coding

In contrast to a single-carrier transceiver, an OFDM transceiver subdivides the channel bandwidth into several smaller chunks and modulates a subcarrier for each one, which allows for concurrent multiuser communications. It also allows the OFDM transmitter to adapt individual subcarriers to localized channel conditions, which provides the transceiver overall with superior performance in terms of interference mitigation, fading, and more. The team worked to create an experimental transceiver design that enables easy transition to a real-world prototyping platform.

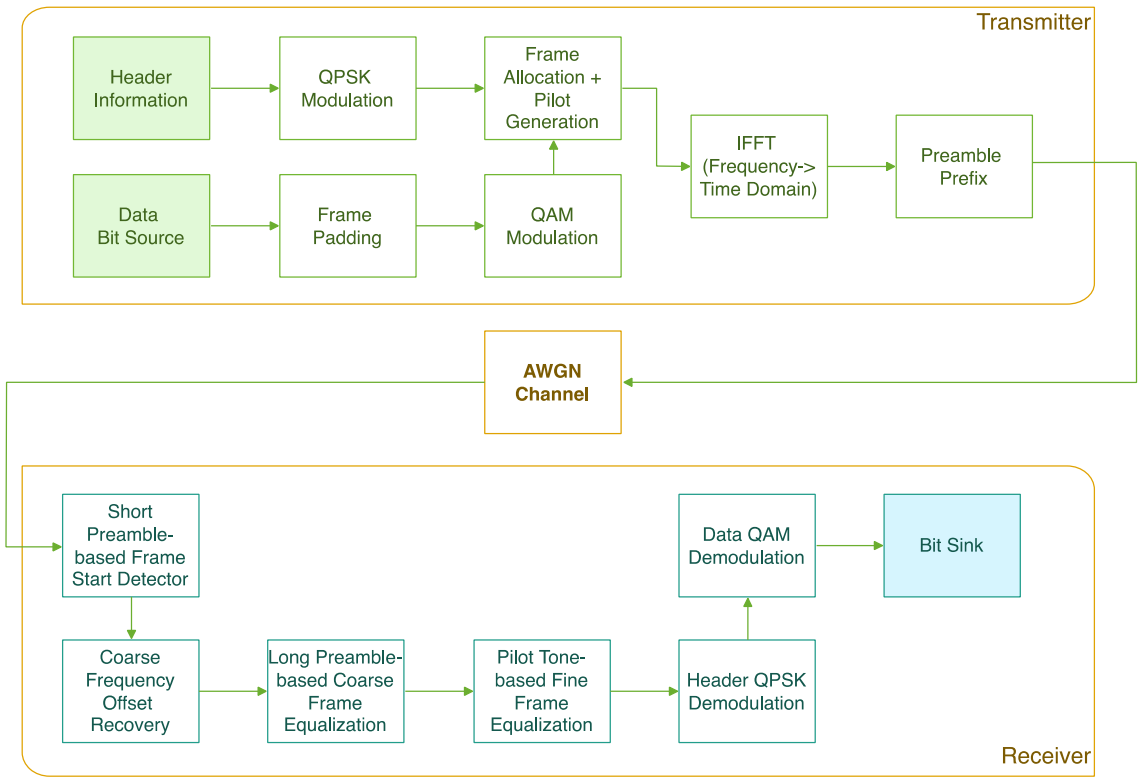

Figure 17. OFDM transceiver design

The team then implemented the design as a MATLAB simulation model and conducted extensive performance evaluations using the path loss models previously established. Results are shown in Figure 18 through Figure 22.

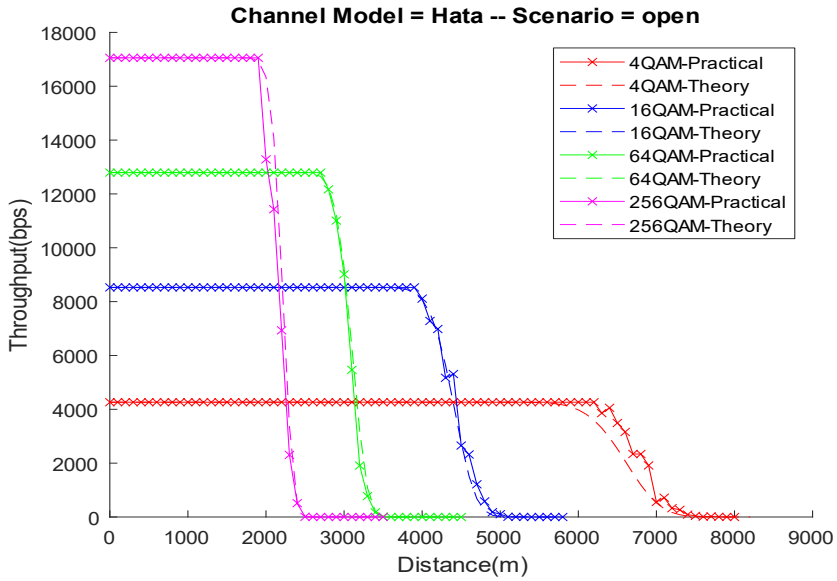

Figure 18. OFDM throughput versus distance for Hata model, open scenario

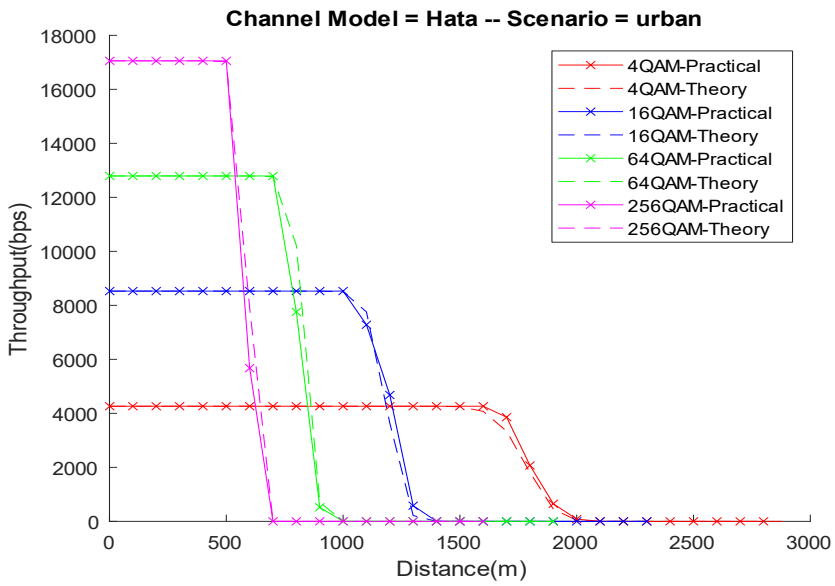

Figure 19. OFDM throughput versus distance for Hata model, urban scenario

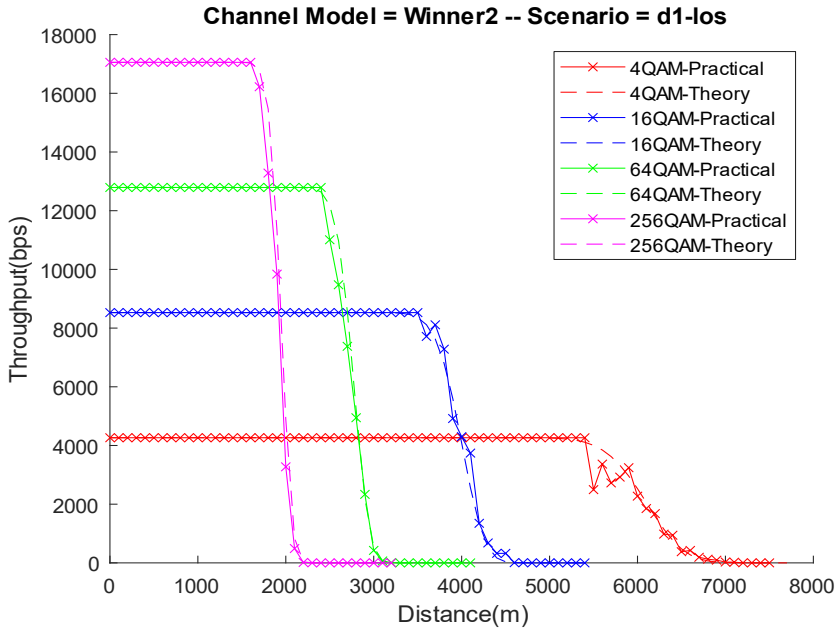

Figure 20. OFDM throughput versus distance for Winner2, D1-LOS (rural open environment)

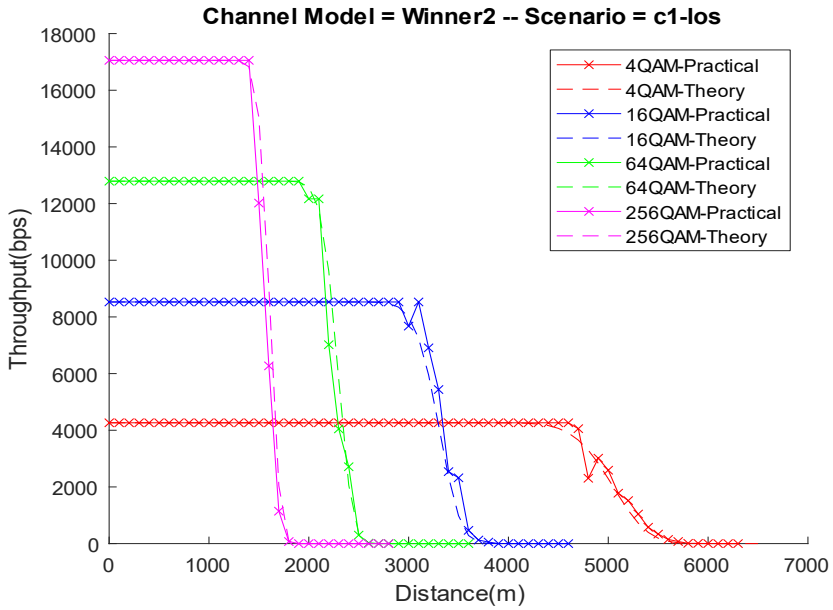

Figure 21. OFDM throughput versus distance for Winner2, C1-LOS (suburban environment)

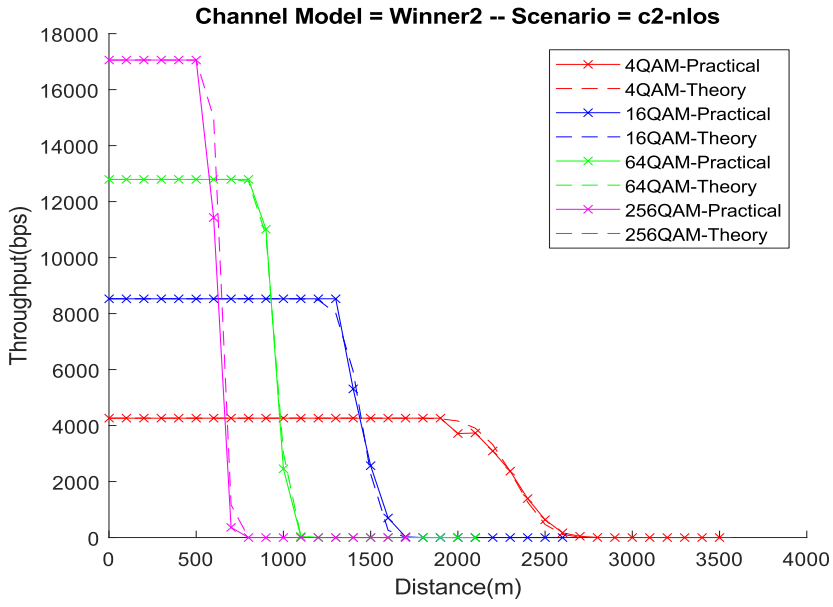

Figure 22. OFDM throughput versus distance for Winner2, C2-NLOS (dense urban environment)

This once again shows a close correlation between the theoretical expected results and the simulation results obtained from the MATLAB model.

9.3 Forward Error Correction Coding Integration with the Transceiver Designs

The design of the single-carrier and OFDM-based transceiver architectures detailed in previous sections each has its pros and cons, and both were considered as potential architectures.

Next, the team incorporated Forward Error Correction (FEC) coding into these architectures. FEC is a way to improve the receive-side bit error rate, and thus communication distance, by sacrificing throughput capacity. The relinquished throughput is instead used to carry additional information that the transmitter inserts into the data stream, often referred to as parity symbols or redundancy symbols. At the receiver side, this additional information is used to detect and correct bit errors. Therefore, by improving the bit error rate as a given SNR, the maximum communication distance can be improved.

The transmitter uses a convolutional coder to process the input bits and produce an encoded bit stream comprised of the convolutional encoder output.

The convolution encoder is comprised of shift registers whose outputs are constructed from the sum of the state of zero, one, or more of these shift registers. The structure is often described using polynomials to represent these connections and the size of the encoder. For example, Figure 23 shows a visual representation of the encoder described by the polynomial matrix [37, 33]. It is important to note that this is in octal notation.

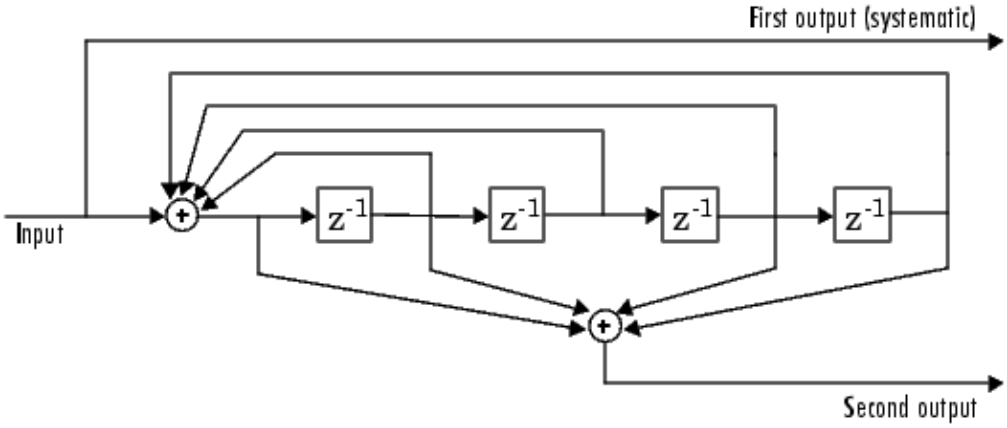

Figure 23. Convolutional encoder example

The relationship between the number of input bits *n* and resulting encoded output bits *k* is represented as a rate *n/k*. The resulting rate can additionally be adjusted through a process called puncturing which essentially removes some of the parity information based on a defined puncture pattern to increase the code rate. This can be used, for example, to convert a rate *1/2* encoder into a rate *3/4* encoder.

The single-carrier transceiver architecture, including the convolutional encoder and decoder stages, is represented in Figure 24.

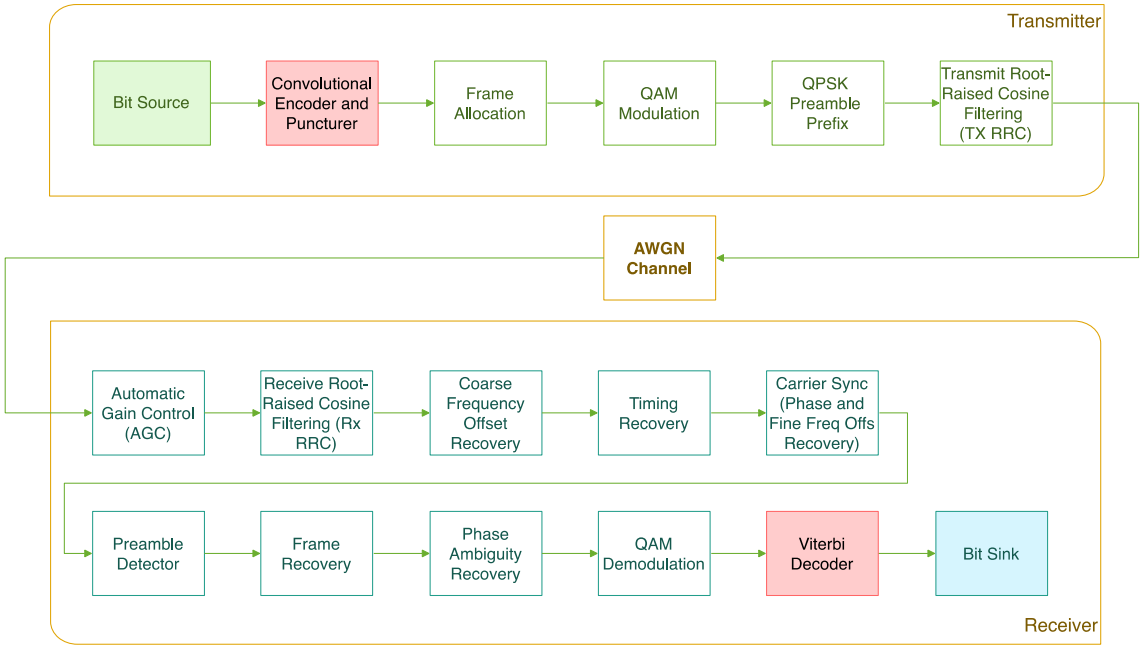

Figure 24. Single-carrier transceiver architecture including the FEC blocks

The new blocks are shown in red. All remaining blocks are the same as in the original single-carrier architecture previously introduced.

Similarly, the OFDM transceiver architecture was updated to incorporate FEC, as shown in Figure 25.

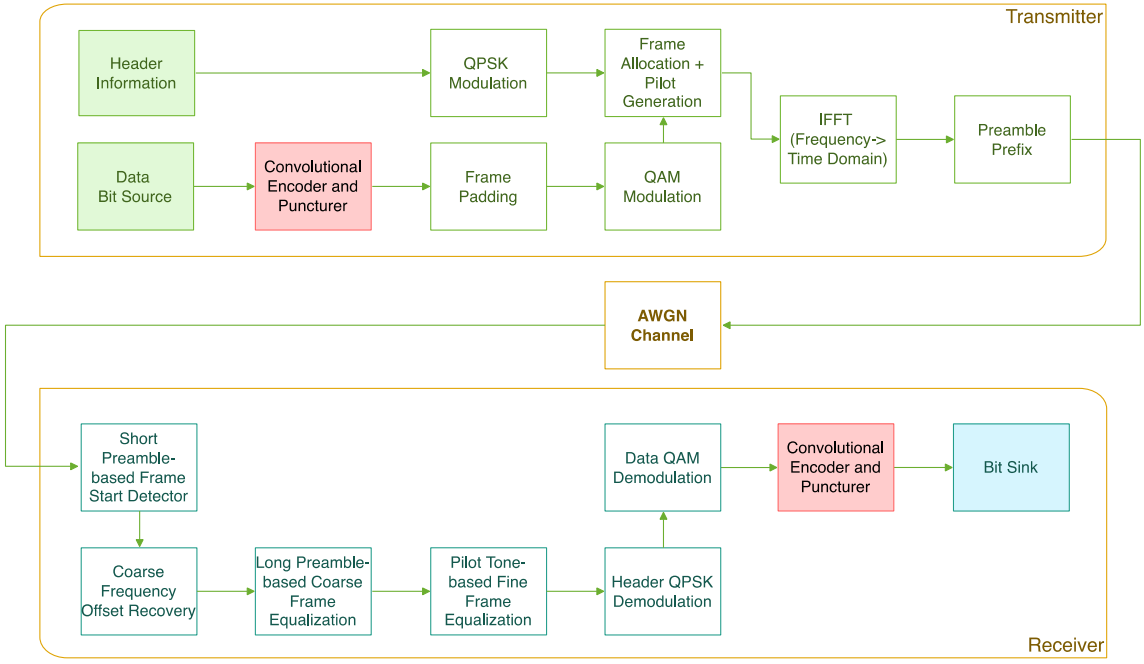

Figure 25. OFDM transceiver architecture including the FEC blocks

The functionality was again implemented in MATLAB and simulated a full transmitter -> channel -> receiver processing flow, including the new convolutional coding processes.

The team first selected an AWGN channel and evaluated the system's Bit Error Rate (BER) versus Eb/N0 performance. For this evaluation researchers considered both the uncoded case, which matches the performance reported in previous quarters, and several different coding rates. The results are shown in Figure 26.

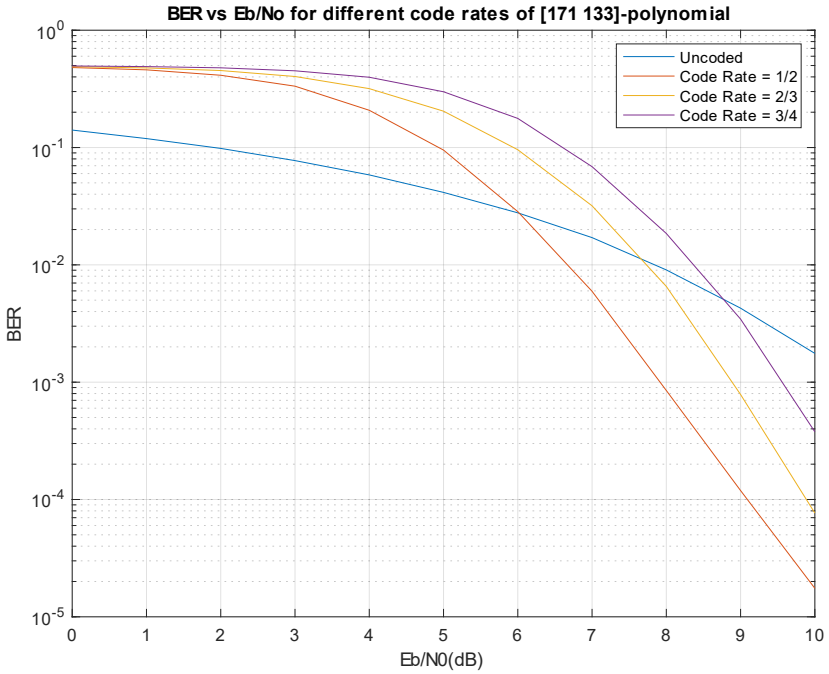

Figure 26. Single-Carrier FEC Performance shown as BER vs Eb/N0

The results validate this implementation as various coding rates show that the more redundant information added, the better the performance gain. The blue line in the graph represents the uncoded transceiver using 16-QAM modulation. The orange line represents the rate 1/2 coded system, which is the system with the highest amount of redundancy. This is followed by the yellow line representing the rate 2/3 transceiver, and finally the purple line showing the rate 3/4 transceiver, which also represents the system with the lowest amount of redundancy information inserted by the convolutional coder and puncturer.

The team then selected several of the propagation models presented in previous reports for the next performance evaluation to obtain insights into how this transceiver will perform under a variety of different channel conditions. Most importantly, achievable throughput at various transmitter-receiver distances was evaluated, which is now also impacted by the convolutional code. Because the convolutional encoder and puncturer essentially expand the volume of the bit stream by inserting redundant bits needed by the receiver to improve bit error rate performance, the capacity of the overall system is effectively reduced. For example, the rate 1/2 encoder doubles the amount of data to be transmitted, which effectively means that throughput for usable data is cut in half. However, due to the capability to repair bit errors at the receiver, the usable communication range can be extended; throughput versus distance performance evaluation results show this relationship. In Figure 27 through Figure 29, results are shown for the Single-Carrier transceiver design, 4-QAM and 256-QAM, and three different channel models. Winner2's D1-LOS model was selected to represent open rural terrain, with virtually no obstructions to the LOS signal path. Two-Ray Ground was also selected as a good representation

of suburban environments, and Winner2's C2-NLOS model represented dense urban environments.

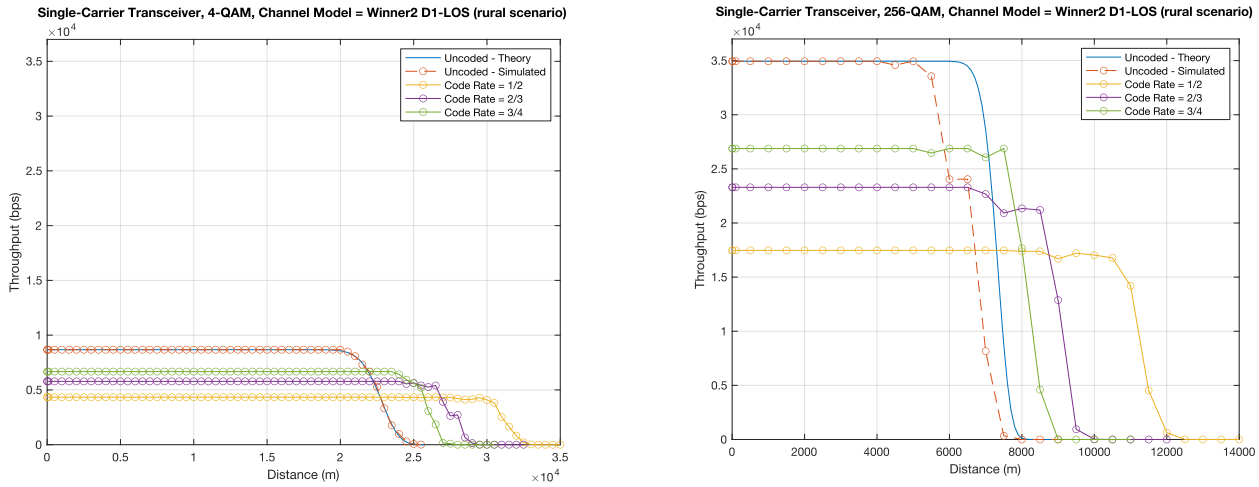

Figure 27. Single-carrier throughput versus distance for Winner2 D1-LOS (open rural environment) model for QPSK and 256-QAM

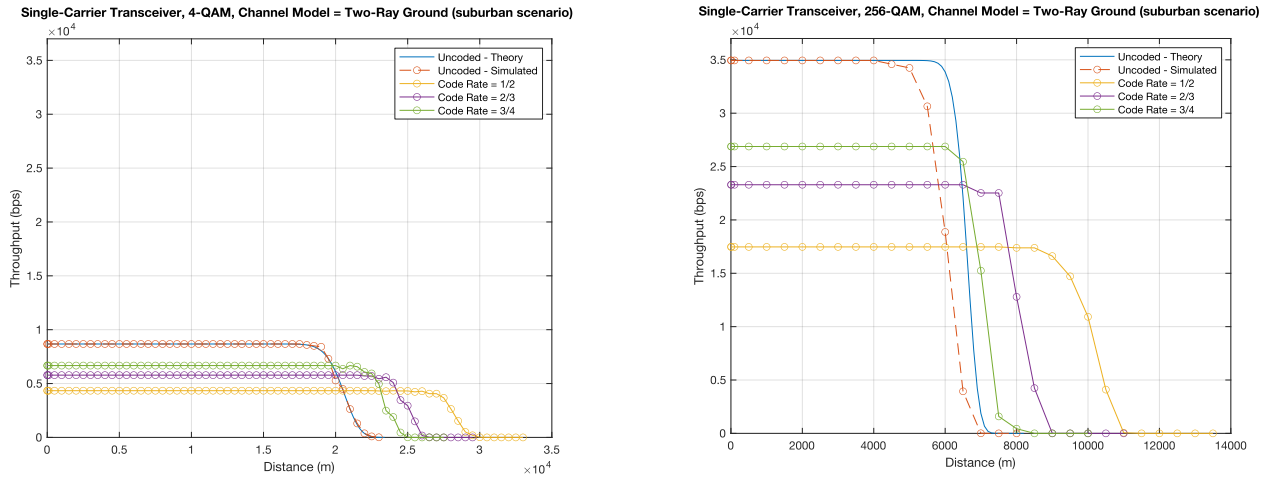

Figure 28. Single-carrier throughput versus distance for the two-ray ground model for QPSK and 256-QAM

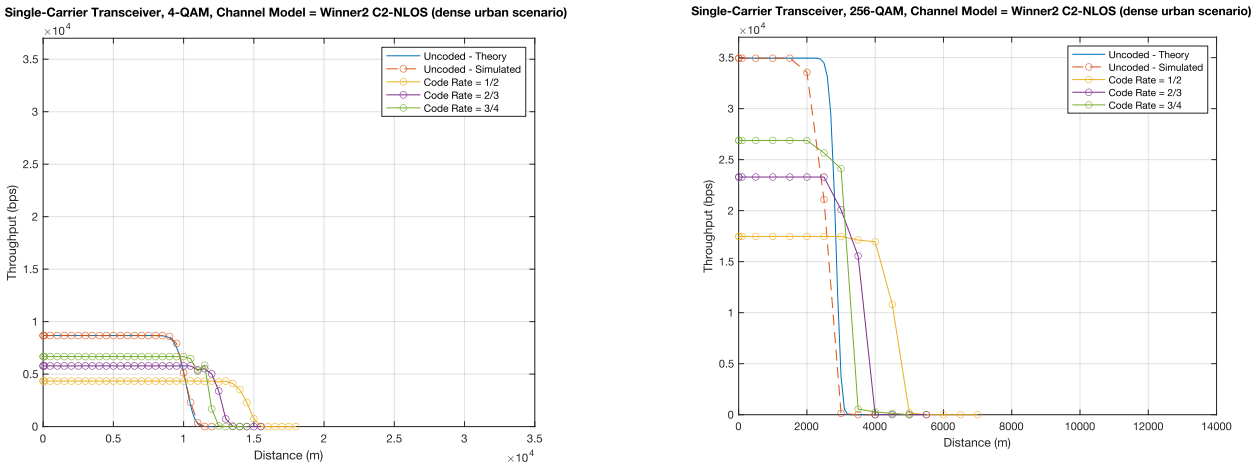

Figure 29. Single-carrier throughput versus distance for Winner2 C2-NLOS (dense urban environment) model for QPSK and 256-QAM

All results were obtained with the 1 W reference power also applied in the path loss model evaluation described in earlier sections and obtained for a 6.25 kHz channel. In each instance, the communication distance increased compared to the uncoded performance. The OFDM results were very similar and therefore not included here.

The communication range of this system was already very high due to the low RF center frequency of 160 MHz. The team leveraged the benefits of the convolutional coder not to further increase communication distance, but rather to improve the reliability of the communication process over the same distance. Due to the limited throughput in this frequency band, the primary application for communications at 160 MHz will be for event-driven communication, such as train approach alerting or PTC communication. Thus, reliability in this case is far more important than communication range. FEC coding achieves this goal.

10. Protocol Stack Design

10.1 Single-Carrier Transceiver Design Selection

Previous sections discussed the design and evaluation of single-carrier and OFDM-based architectures. However, for the protocol stack design and evaluation, the team concentrated on the single-carrier design only. This selection was driven by several factors, especially the fact that OFDM incurs significantly higher overhead, which in turn drastically limits the available higher-layer throughput. The single-carrier scheme still provides a variety of multiple-access methods, which would allow the system to provide point-to-multipoint services. The team plans to further investigate OFDM and explore different schemes for overhead reduction in Phase 4.

10.2 Protocol Stack Details

Earlier sections describe significant details of the physical layer, arguably one of the most important aspects in any transceiver design. It sets the stage for any higher-layer functionality, as well as overall performance capabilities.

Once the physical layer (PHY) was established, the design then focused on the protocol layers built on top of it. Figure 30 shows the layers considered and realized in the design.

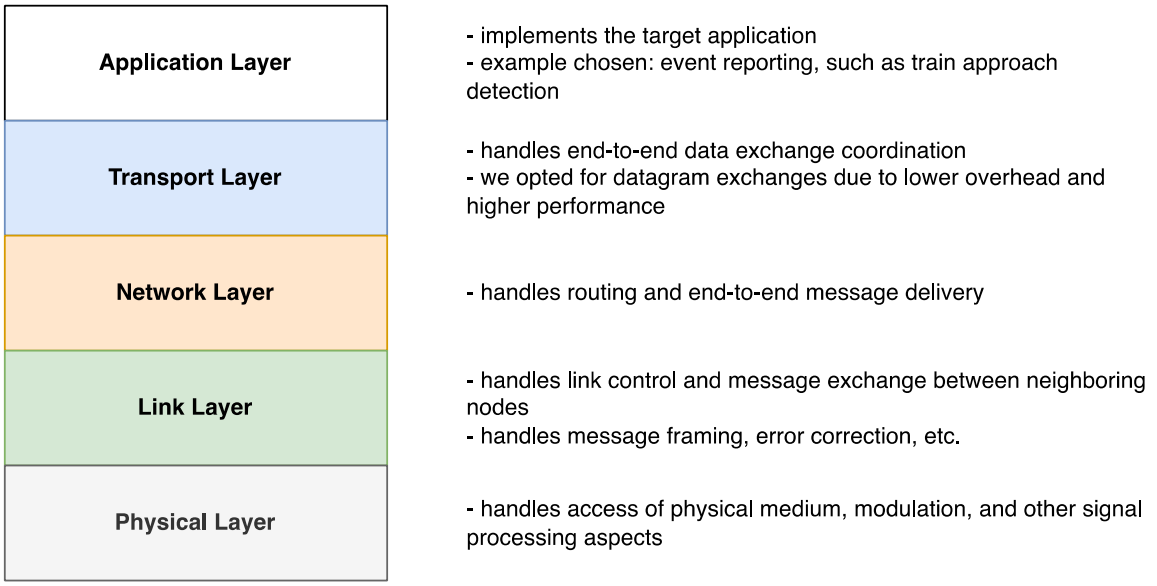

Figure 30. Protocol stack design used for 160 MHz study

As shown in the figure, each layer of the protocol stack has specific responsibilities, which is the core premise of a layered approach. The functionality of a higher layer is built upon using the services provided by a lower layer.

In this design, the team focused on five of the seven layers of the OSI reference architecture. In the OSI model, two additional layers, Session and Presentation, are present between the transport and application layer. On this more streamlined architecture the focus was solely on layers 1 (Physical), 2 (Link), 3 (Network), 4 (Transport), and 7 (Application) from the OSI reference model. Within the applications of interest for using 160 MHz RF, the team found no compelling reason to include the extra services provided by the Session and Presentation layers.

In a layered approach to networking, services build on top of each other. Each protocol within a given layer usually includes additional message fields that enable it to perform its operations. These additional fields are grouped together in the header structure included by that layer, in addition to the payload it is transporting for the layer above it, and potentially additional protocol element fields after the payload, in what is called the footer.

Although vital to the communication operations, header and footer fields are used to communicate information that is not application data. Therefore, this overhead reduces the total possible application data throughput. When designing protocols, it is therefore important to minimize as much as possible the incurred overhead. The team spent considerable time designing and revising the protocols presented below, as well as their protocol elements. However, there likely is room for additional improvements, which the team hopes to identify through more implementations of real-world applications in subsequent project phases.

10.3 Physical Layer

The PHY layer focuses on modulating the information bits provided by the link layer (layer 2), into information symbols, which the radio then turns into waveform samples. On the receiver side, signal processing is performed to recover the start and end of this sequence of waveform samples, and in what is essentially the reverse of the operation on the transmitter side, the information bits are recovered and provided to the receiver's link layer for further processing.

The study architecture supports QAM, one of the most prominent modulation schemes in wireless communications. It supports multiple modulation orders, ranging from 2-QAM to 256-QAM. The higher the modulation order, the more information bits are grouped together and transferred by a single symbol. In 2-QAM, 1 bit is represented by 1 symbol, whereas in 256-QAM, 8 bits are represented by 1 symbol. There is a correlation between density (the number of bits per symbol) and the resulting robustness against noise and interference. The lower the density (for example 2-QAM), the higher the robustness. However, since the number of symbols is limited by the fixed channel bandwidth, the lower the density, the lower the maximum throughput is as well; there is an inverse correlation between throughput and distance for each modulation order within QAM. 256-QAM provides the best throughput but is limited in distance. 2-QAM provides far better communication range, but at the expense of throughput.

This correlation is exploited by the adaptive modulation and coding scheme selection. An increase in distance between transmitter and receiver results in an increase in path loss (i.e., the measure of the reduction in signal strength in the signal that was generated at the transmitter and observed at the receiver). The receiver also incurs noise, predominantly thermal noise, that impacts the signal, as well as interference that results from other transmitters. Based on channel conditions, in particular the SNR power ratio observed at the receiver, the transceiver system will adapt the modulation and coding scheme to maximize throughput while also achieving reliable communication for the given channel conditions.

10.4 Link Layer

The link layer uses the PHY layer to transmit and receive data frames. The framing wraps the packetized information received from layer 3 (network layer) into frames, by prepending information including the source and destination node address, frame type and length, as well as a framing indicator, which consists of the preamble sequence as well as the MCS indicator field. Table 10 lists the currently defined MCS indices and their respective meaning. These entries are

not all consecutive; the gaps within the numbering allow for the addition of support for additional coding schemes or rates within each QAM modulation and adds support for additional modulation schemes in the future. The MCS index field provides a total numbering space from 0 to 255.

Table 10. MCS Index Assignments List

Modulation Scheme	Coding	Coding Rate	Assigned MCS Index
2-QAM (BPSK)	Convolutional Coding	1/2	2
2-QAM (BPSK)	Convolutional Coding	2/3	3
2-QAM (BPSK)	Convolutional Coding	3/4	4
4-QAM (QPSK)	Convolutional Coding	1/2	12
4-QAM (QPSK)	Convolutional Coding	2/3	13
4-QAM (QPSK)	Convolutional Coding	3/4	14
16-QAM	Convolutional Coding	1/2	22
16-QAM	Convolutional Coding	2/3	23
16-QAM	Convolutional Coding	3/4	24
32-QAM	Convolutional Coding	1/2	32
32-QAM	Convolutional Coding	2/3	33
32-QAM	Convolutional Coding	3/4	34
64-QAM	Convolutional Coding	1/2	42
64-QAM	Convolutional Coding	2/3	43
64-QAM	Convolutional Coding	3/4	44
128-QAM	Convolutional Coding	1/2	52
128-QAM	Convolutional Coding	2/3	53
128-QAM	Convolutional Coding	3/4	54
256-QAM	Convolutional Coding	1/2	62
256-QAM	Convolutional Coding	2/3	63
256-QAM	Convolutional Coding	3/4	64

Both elements of the framing indicator are always transmitted using BPSK modulation without error correction coding. This fixed representation allows the receiver to detect the frame start and discover the MCS scheme in use for the remainder of the transmitted frame information.

The link layer also performs Carrier Sense Multiple Access with Collision Avoidance (CSMA/CA) based on the mechanism used in IEEE 802.11 (WIFI). It uses a Distributed Control Function (DCF) built upon a Distributed Coordination Function (DCF) Inter-Frame Spacing (DIFS) of 260 microseconds and a slot duration of 50 microseconds.

Addressing uses node addresses that are 16 bits long.

10.5 Network Layer

The network layer allows end to end message transmissions through routing. Routing protocols were not specified in the initial protocol architecture. However, further investigations will be conducted as part of ongoing efforts in the next project phase.

Network address also uses the node address format of 16 bits.

10.6 Transport Layer

In the initial architecture the team focused on minimizing control overhead and opted for a datagram-based approach for the initial protocol stack design; the team plans to also design and evaluate a stream-based session design in a later revision. This initial design, given the resource-limited nature of communications at 160 MHz, opted to use 4-bit port identifiers, for a total of 16 active application instances supported by the system. Additional research and discussions with railroad stakeholders will allow for the adjustment of these initial assumptions in the next phase.

10.7 Application Layer

The team opted to focus on train approach detection for initial simulation-driven evaluation, and more specifically, to implement an event notification that would provide services for alerting workers within an area of an approaching train.

To that end, the application layer protocol specifies a priority flag and an event type field to accommodate different types of notifications (e.g., “train approaching,” “train dangerously close,” “train departing,” and “train departed”). The application layer message can also incorporate additional event-specific information in its payload section. This provides for great flexibility to adapt to different situations and application needs.

10.8 Protocol Header Structure

Figure 31 shows the current protocol header elements.

- The framing indicator occupies 24 bits, always transmitted using BPSK modulation without error correction coding.
- The link layer frame overhead is 64 bits.
- The network layer packet overhead is 56 bits.
- The transport layer datagram overhead is 24 bits.
- The application layer message overhead is 24 bits.

This amounts to a total overhead of 168 bits, not including the framing indicator. Additional research work is planned for Phase 4 of this effort, in conjunction with the software radio implementation, to further reduce this overhead amount.

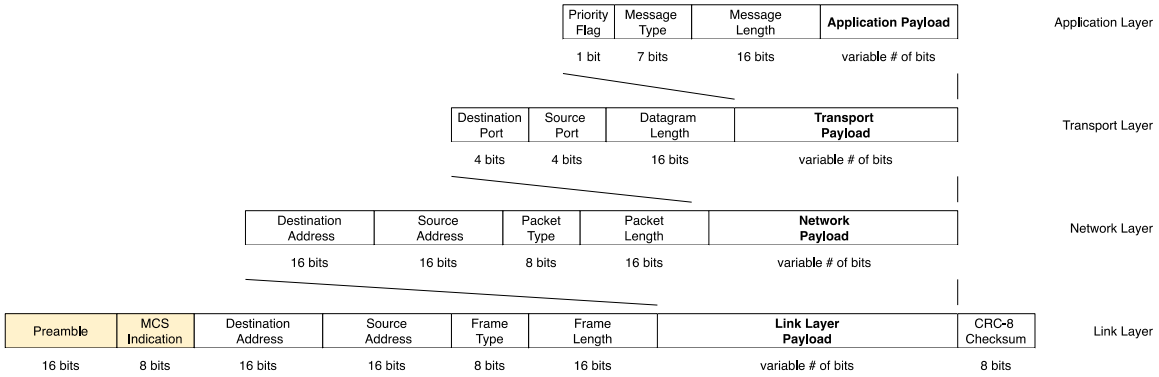

Figure 31. Protocol layers and their header elements

11. Event-Driven Protocol Stack Simulation

To evaluate the end-to-end performance of the full protocol stack design, the team implemented this protocol into an event-driven simulation framework within MATLAB.

The framework implements a central, globally shared event scheduler and dispatcher, as well as a global RF state manager, and it implements each simulated node with all their protocol stack layers. Event generation parameters for each node can be precisely controlled, including start time and duration, event intervals or distribution, and event destinations.

The node protocol implementations are responsible for all message processing, including queuing, framing, and error handling. The PHY layer uses the previously obtained results of the bit error rate for different channel models and channel conditions to perform lookup operations to determine each received frame's bit error rate. It then determines whether the frame was correctly received, sending it upwards through the receiver's protocol stack, or discarded due to remaining bit errors that could not be corrected by the error correction coding.

12. Simulation Scenarios and Performance Results

Several simulation scenarios intended to establish baseline parameters were designed for this project. All these scenarios used a simple 2 node simulation setup, where the first node generates and transmit events to the second node.

12.1 Noise Floor and Noise Figure Considerations

The driving factor for transceiver performance is the condition of the RF channel, in particular the SNR. The received signal power is the result of the transmit power, the transmit and receive antenna gains, and the path loss. The path loss represents the amount of attenuation applied to a signal by the time the signal reaches the receiver; the larger the distance, the larger the path loss. Channel models capture how the environment influences that path loss, which can range from an ideal free-space environment without any obstacles between sender and receiver to a heavily cluttered metropolitan area, where buildings, vehicles, and many other objects often interfere with signal propagation.

The noise observed by the receiver is another key factor in determining SNR. This noise, in particular the noise floor, are key in determining the amount of receiver noise power. The noise floor is primarily driven by the bandwidth of the receiver, known as the detection bandwidth; only the amount of noise power within the detection bandwidth will be incurred by the receiver. In very narrow 6.25 kHz channels, there is significantly less noise power than in receivers at, for example, 2.4 GHz for WIFI observed with a 20 MHz channel width.

Consequently, the theoretical noise floor for a 6.25 kHz channel at a 290 K environment temperature is -136 dBm, assuming the receiver has ideal hardware components. Typical receivers fail to realize the theoretically possible noise floor, however, and instead incur additional noise due to hardware imperfections or digital signal processing artifacts. This degradation is expressed as the receiver's "noise figure" (NF), or the additional noise, expressed in dB, incurred by the receiver. For study simulation, the team gave the receiver an NF of 26 dB, which results in an overall receiver noise power of -110 dBm. High-quality RF receiver implementations typically achieve a ~10 dB NF; the study's NF puts the simulated receiver more in line with a software radio implementation or lower-quality transceiver hardware.

12.2 Scenario 1: End-to-End Latency

In this scenario, there are only two nodes, with a dedicated transmitter and a dedicated receiver, so this simulation does not produce any interference. It also does not produce any contention for the RF channel. This allowed the team to determine the best possible end-to-end latency over the range of communication distances supported by this transceiver architecture.

For end-to-end latency the team considered message processing, queuing, the DCF for multiple access, message transmission duration, and the propagation delay for the radio signal to reach the destination. Given the relatively narrow channel with limited bandwidth, the transmission duration was expected to be the dominant factor in the overall end-to-end latency. However, this is only true for scenarios with no or low contention. For highly contentious environments with multiple nodes within RF range of each other, the contention mechanism through the DCF is also expected to produce a significant latency.

Figure 32 shows the end-to-end latency for different distances between nodes 1 and 2. Each simulation contained at least 1,000 events to be communicated.

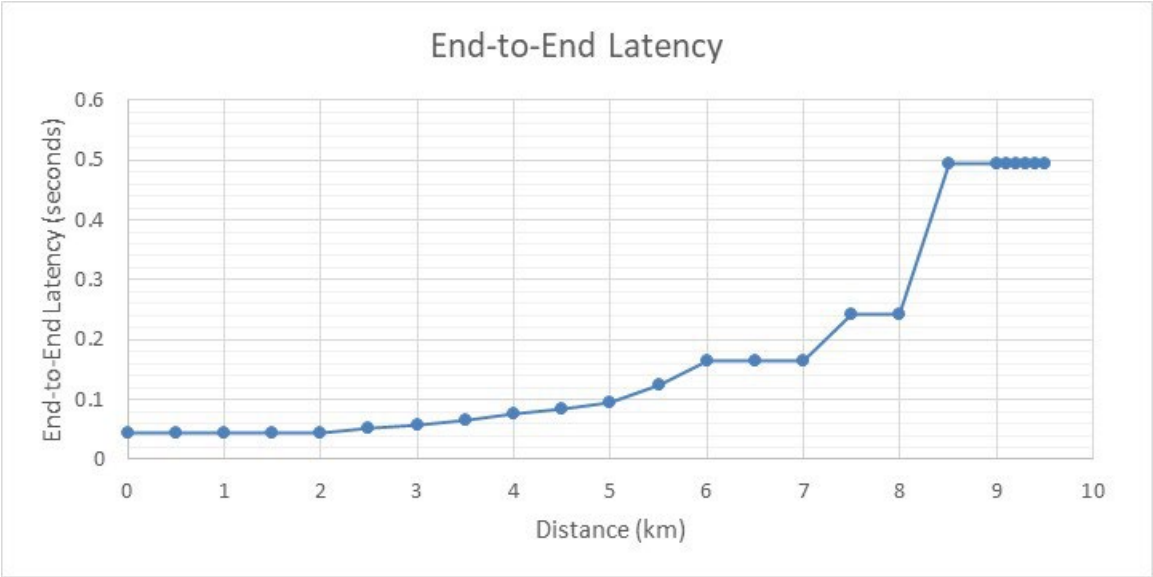

Figure 32. End-to-end latency versus node distance

Over these different simulated communication distances, the selected MCS type was studied and tracked. This was expected to change from 256-QAM with coding rate 3/4, which represents the highest-throughput MCS scheme with the least robustness to noise, and to change increasingly toward a more robust scheme with lower throughput potential, until reaching BPSK, rate 1/2, which is the most robust available scheme with the lowest throughput potential.

This change in MCS scheme is shown in Figure 33.

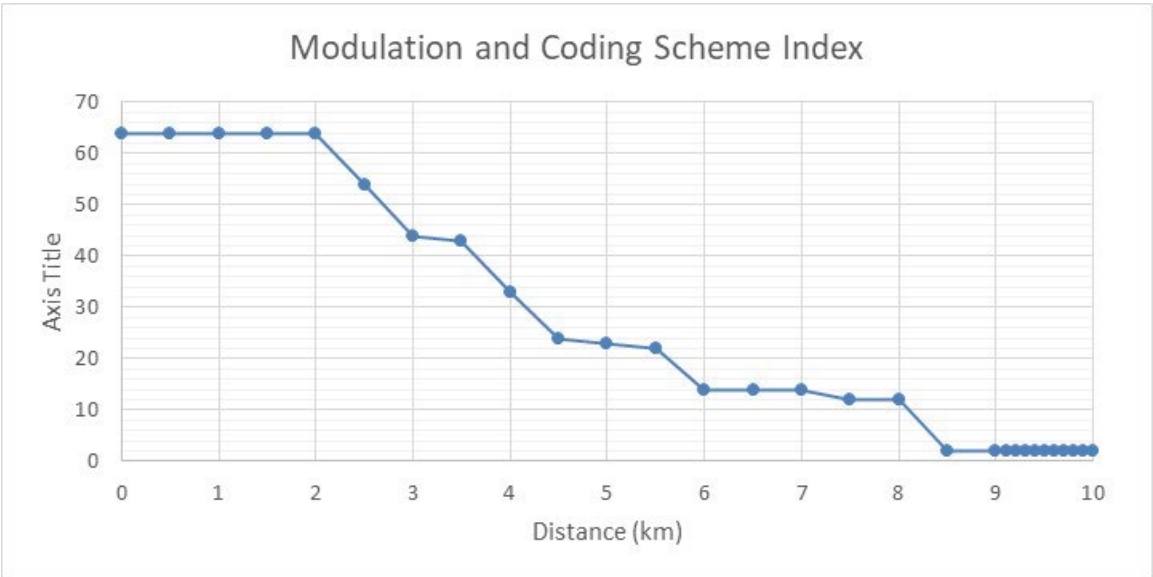

Figure 33. Modulation and coding scheme adaptation over distance

12.3 Scenario 2: Packet Loss Rate

Packet loss rate (PLR) is another key metric in RF communication schemes. Packet loss is primarily the result of bit errors incurred when the SNR degrades. In each MCS scheme, degrading SNR causes the BER to increase until it reaches levels that no longer allow for successful transmission of packets. The levels of SNR at which successful reception deteriorates is different for each MCS scheme, which in turn gives rise to adaptive selection of the most appropriate MCS scheme for each SNR value over the RF communication range of a transceiver system. The maximum communication range is reached when even the most robust MCS scheme fails to provide successful packet reception.

To study this behavior in the simulation, the team conducted a sweep over the RF communication distance between nodes 1 and 2 and at each step monitored the packet loss rate. The team expected to see low to no packet losses for most of the communication range, given the correct selection of MCS schemes to suit the SNR at that communication distance. Only at the very edge of the communication range did the team expect to observe a rapid deterioration in PLR from 0 percent (all packets succeed) to 100 percent (all packets fail to be received), as shown in Figure 34.

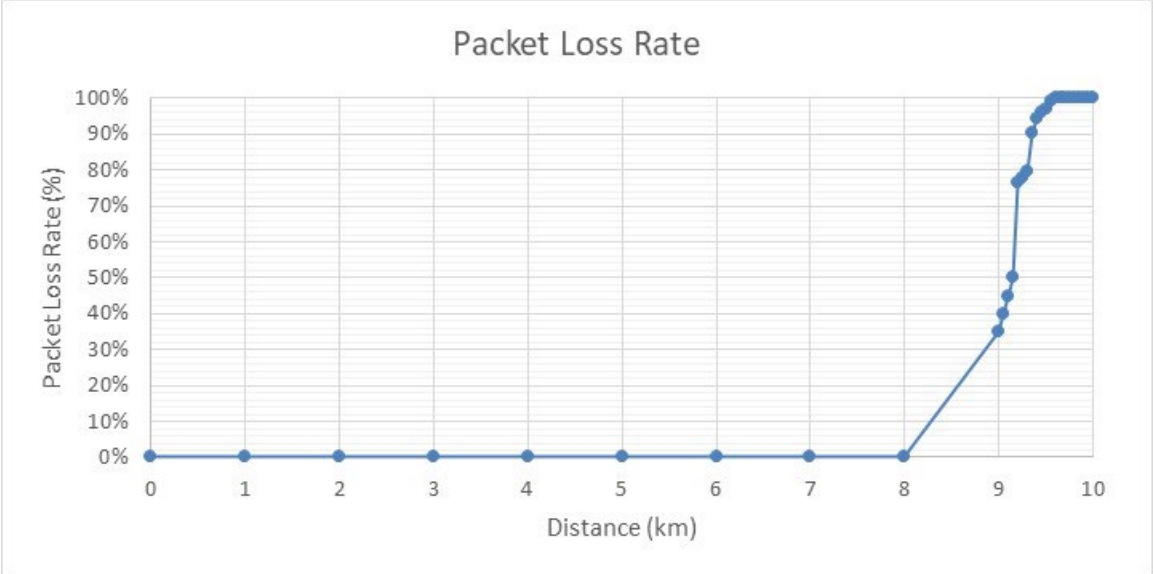

Figure 34. Packet loss rate over distance

12.4 Scenario 3: End-to-End Application Layer Throughput

The final baseline scenario studied the resulting end-to-end throughput at the application layer. Sometimes also referred to as goodput, this throughput is the resulting bit stream received after discarding any failed messaged due to bit errors, as well as the removal of all lower layer protocol overhead information. Rather than counting all bits received, as is the case with the layer 2 throughput, this throughput focuses only on the successfully received application layer messages.

A sweep over the communication distance was again performed. With MCS adaptation the team expected a step-wise degradation in end-to-end application layer throughput. This is the result of the step-by-step switching from low-robustness, high-throughput MCS schemes down to highly

robust, low-throughput MCS schemes. This illustrates the inherent tradeoff between distance and performance, as shown in Figure 35.

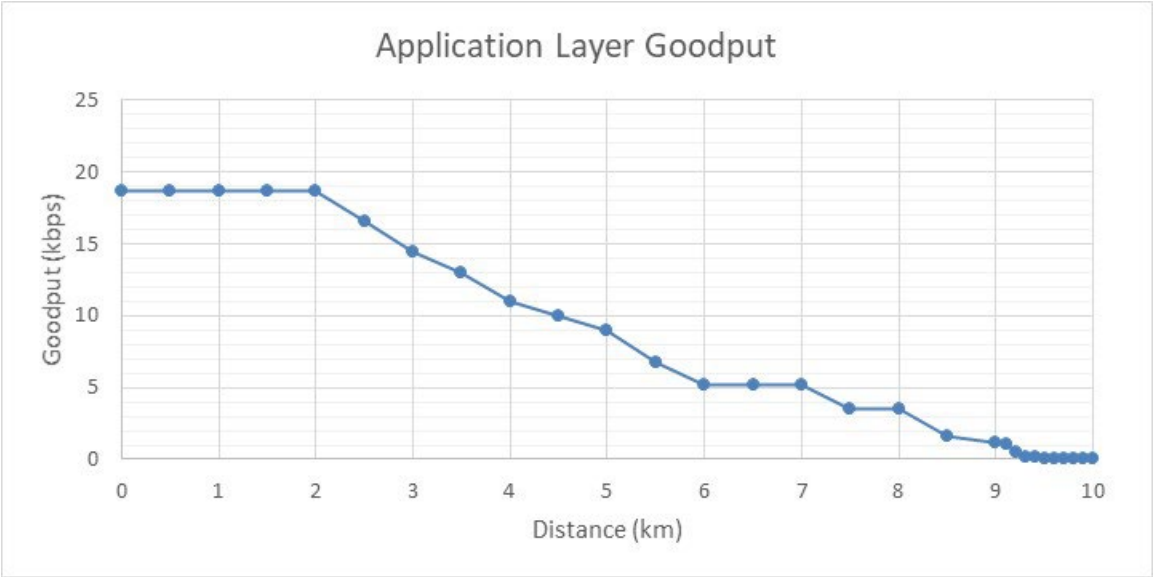

Figure 35. Application layer goodput over distance

Figure 36 plots the layer 2 throughput.

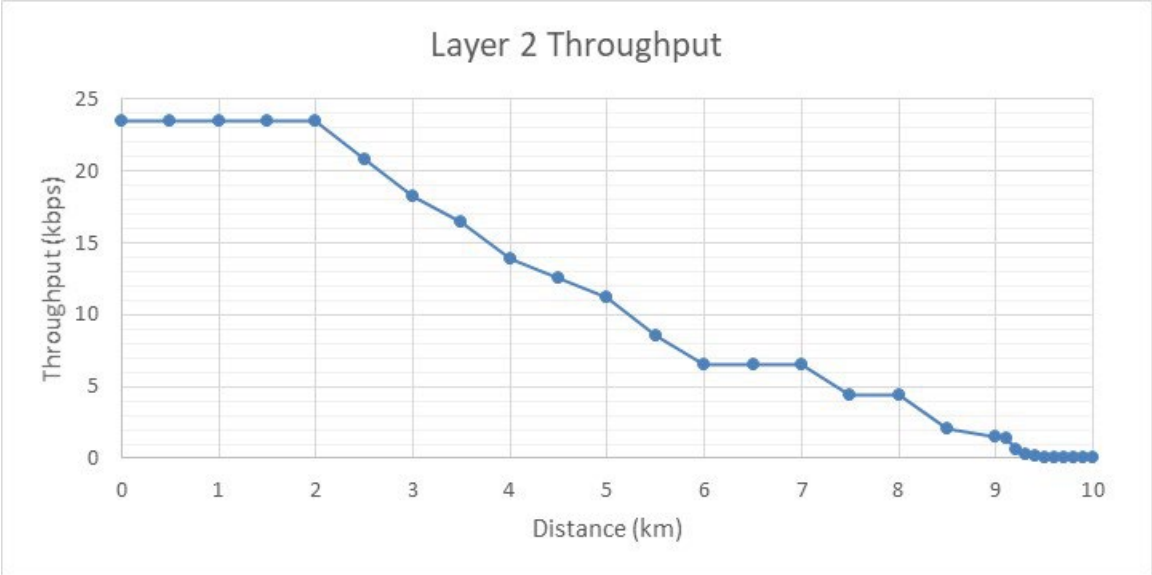

Figure 36. Layer-2 throughput over distance

End-to-end throughput is higher at all distances compared to the application layer. This was expected, as the number of received messages is unchanged, but at layer 2 the throughput includes far more protocol header bits from the various protocol layers than at the application layer. This can best be observed in Figure 31, which shows the protocol layers and their protocol elements.

12.5 Radio Horizon Considerations

The studied scenarios show that the maximum communication distance is approximately 10 km. To verify the feasibility of this distance, the team also considered what is known as the radio horizon, or the distance from an elevated antenna to the horizon that results from the earth's curvature. This means that at some far point, receiver antennas would appear below the horizon and therefore cannot receive a transmitted signal. Further elevating the antenna would increase the radio horizon, so when dealing with long-range wireless systems, it is important to consider the radio horizon resulting from different antenna heights. In this study of the 160 MHz radio system, antenna heights were expected to be at most the height of a typical diesel locomotive (i.e., approximately 16 feet, or 5 meters). As the approximate radio horizon for a 5 meter antenna is about 9.2 kilometers, the simulated maximum communication distances are in line with the maximum achievable distance due to radio horizon limits.

13. Conclusions and Future Work

Throughout this third phase of researching wireless communications architectures for rail service, the team focused on developing an approach that will allow railroads to alleviate significant challenges in their continued adoption of wireless solutions due to RF spectrum scarcity. Without adequate RF spectrum, wireless solutions cannot continue to expand, while existing resources tend to be overtaxed or are expensive to license.

Efforts focused on exploring underused RF bands, as well as bands that are abandoned or only support legacy applications. These RF bands are prime candidates to be re-used and re-envisioned for modern wireless applications. The 160 MHz RF band was used as a case study in this effort.

The team conducted extensive regulatory requirements reviews and theoretical performance evaluations, designed a suitable transceiver architecture, developed a full protocol stack for the architecture, and conducted a computer-simulation-driven performance evaluation. During the performance evaluation, dozens of simulation scenarios were designed, simulated, and processed, providing metrics for end-to-end latency, packet loss rate, and application layer goodput for full transceiver architecture and protocol stack. The results and insights from this study appear to be very promising.

Several publications [65-71] were developed throughout this project phase to disseminate the findings to the railroad community and the scientific community at large and the team continues regular engagement with rail industry stakeholders through biweekly conference calls and progress updates.

These findings set the stage for the next project phase, which will focus on the design and development of a universal software radio framework for the rail industry. The 160 MHz design will be used as a case study to realize the transceiver design as a fully featured implementation that will then be used for real-world field testing.

14. References

[1] H.R.6003 - 110th Congress (2007-2008): Passenger Rail Investment and Improvement Act of 2008. (2008, June 12).

[2] PRIIA Section 305 Statute, American Association of State Highway Transportation Officials (AASHTO).

[3] Spectrum Management.

[4] United States Frequency Allocations (2016). US Department of Commerce.

[5] Ramos, A., Gacnik, J., Anaya, R., Gonzalez, A., Brosseau, J., Gage, S., & Polivka, A. (2020). *Railroad Wireless Communications Roadmap* (Report No. DOT/FRA/ORD-20/10). Federal Railroad Administration.

[6] Reallocation assessment of 30-50 MHz (n.d.). National Telecommunications and Information Administration.

[7] Very High Frequency (VHF).

[8] 30 MHz to 50 MHz (2022). FCC ID Database.

[9] Railroad Radio Service, 47 CFR § 90.91 (1996).

[10] Frequency Plan (2021). Association of American Railroads.

[11] Bandara, D., Abadie, A., Melaragno, T., & Wijesekara, D. (2014). Providing Wireless Bandwidth for High-Speed Rail Operations. *Procedia Technology, 16*, 186-191.

[12] Buzid, T. (2004). Modulation Choices for Telemetry Transmitters and Receivers. *Microwaves & RF*.

[13] RCL-II Locomotive Remote Control System Operating Instructions (2015). Laird.

[14] Craven, P. & Oman, P. (2008). Simulation Of Advanced Train Control Systems. In: Papa, M., Shenoi, S. (eds) *Critical Infrastructure Protection II. ICCIP 2008. The International Federation for Information Processing, vol 290*. Springer, Boston, MA.

[15] Power and Antenna Height Limits, 47 CFR § 90.205 (1995).

[16] Human Exposure to Radio Frequency Fields: Guidelines for Cellular Antenna Sites (2019). Federal Communications Commission.

[17] Numerical Electromagnetics Code.

[18] Momentum (electromagnetic simulator).

[19] Ansys HFSS.

[20] Tzoulis, A. (2009). *Numerical Modeling of Electromagnetic Problems with the Hybrid Finite Element - Boundary Integral - Multilevel Fast Multipole - Uniform Geometrical Theory of Diffraction Method*. (Dissertation) Vom Fachbereich Elektrotechnik und Informationstechnik der Technischen Universit at Darmstadt.

[21] XFdtd.

[22] AWR Axiem. Cadence.

[23] JCMsuite.

[24] COMSOL Multiphysics.

[25] FEKO.

[26] Elmer FEM solver.

[27] Cisco Packet Tracer Data Sheet. Cisco.

[28] Varga, A. (2019). A Practical Introduction to the OMNeT++ Simulation Framework. In: Virdis, A., Kirsche, M. (eds) *Recent Advances in Network Simulation. EAI/Springer Innovations in Communication and Computing*. Springer, Cham.

[29] Varga, A. & Hornig, R. (2008). An Overview of the OMNeT++ Simulation Environment. In: *Proceedings of the 1st International Conference on Simulation tools and Techniques for Communications, Networks and Systems & Workshops (Simutools '08)*. Institute for Computer Sciences, Social-Informatics and Telecommunications Engineering, Brussels, BEL, Article 60, 1–10.

[30] NetSim Network Simulator. Boson.

[31] GNS3.

[32] Cisco Virtual Internet Routing Lab (VIRL PE). Cisco Learning Network.

[33] EVE-NG.

[34] OPNET.

[35] Open-Source Network Simulators/Emulators (2021). *Open-Source Routing and Network Simulation Blog.*

[36] NS-3 Network Simulator. NS-3.

[37] Antidote. NRE Labs.

[38] Cloonix Documentation.

[39] Ahrenholz, J., Danilov, C., Henderson, T. R. & Kim, J. H. (2008). CORE: A real-time network emulator, *MILCOM 2008 - 2008 IEEE Military Communications Conference*, *2008*, 1-7.

[40] Integrated Multiprotocol Network Emulator/Simulator (IMUNES). University of Zagreb.

[41] Mininet. Mininet Project Contributors.

[42] Shadow.

[43] Virtual Networks over linuX (VNX).

[44] Volcano 5G. Siradel.

[45] S_5GChannel for Advanced 5G mmW propagation modeling. Siradel.

[46] MATLAB. MathWorks.

[47] AN Codes.

[48] Roth, R. M. & Seroussi, G. (1988). Encoding and decoding of BCH codes using light and short codewords. In: *IEEE Transactions on Information Theory*, *34*(3), 593-596.

[49] Berger Code.

[50] Tian, C., Vaishampayan, V. A., & Sloane, N. J. A. (2007). Constant weight codes: a geometric approach based on dissections. arXiv:0706.1217.

[51] Tahir, B., Schwarz, S., & Rupp, M. (2017). BER Comparison between Convolutional, Turbo, LDPC, and Polar Codes. *2017 24th International Conference on Telecommunications (ICT)*, pp. 1-7.

[52] Saranurak, T. & Wang, D. (2019). Expander decomposition and pruning: Faster, stronger, and simpler. *Proceedings of the Thirtieth Annual ACM-SIAM Symposium on Discrete Algorithms*. Society for Industrial and Applied Mathematics, pp.2616-2635.

[53] Binary Golay code.

[54] Goppa code.

[55] Horadam, K. J. (2007). *Hadamard Matrices and Their Applications*. Princeton University Press.

[56] Buddha, S. K. (2011). Hamming and Golay Codes.

[57] Error Correcting Codes.

[58] Long code (mathematics).

[59] Moision, B. (2013). Decoding complexity and performance of short-block LDPC codes over GF(q). *IPN Progress Report*, *42-194*, 1-16.

[60] Eldin, A.G., Hassan, A., Dessouky, M.I., Abouelazm, A., & Shokair, M. (2012). Evaluation of complexity versus performance for turbo code and LDPC under different code rates. Proceedings of SPACOMM 2012, 93-98.

[61] Wicker, S. B. & Bhargava, V.K., eds. (1999). Reed-Solomon Codes and Their Applications. Wiley-IEEE Press.

[62] Abbe, E., Shpilka, A., & Ye, M. (2021). Reed–Muller Codes: Theory and Algorithms. *IEEE Transactions on Information Theory, 67*, 3251-3277.

[63] Rosenqvist, T. & Sloof, J. (2019). Implementation and Evaluation of Polar Codes in 5G. (Dissertation) Karlstad University.

[64] IST-4-027756 WINNER II D1.1.2 V1.2 WINNER II Channel Models (2007). Information Society Technologies.

[65] Ghasemzadeh, P., Hempel, M., & Sharif, H. (2021). A Novel High-Accuracy Low-Execution Time Machine Learning- Driven Approach to Automatic Modulation Classification. *2021 IEEE 18th Annual Consumer Communications & Networking Conference (CCNC)*, 1-6.

[66] Ghasemzadeh, P., Hempel, M., Banerjee, S., & Sharif, H. (2021). A Spatial-Diversity MIMO Dataset for RF Signal Processing Research. *IEEE Transactions on Instrumentation and Measurement*, *70*, 1-10.

[67] Ghasemzadeh, P., Hempel, M., & Sharif, H. (2022). GS-QRNN: A High-Efficiency Automatic Modulation Classifier for Cognitive Radio IoT. *IEEE Internet of Things Journal, 9*(12), 9467-9477.

[68] Ghasemzadeh, P., Hempel, M., Sharif, H., & Omar, T. (2022). Maximizing RF Communications Throughput for Railroad Applications at 160 MHz. *Proceedings of the 2022 Joint Rail Conference*. ASME.

[69] Ghasemzadeh, P., Hempel, M., Sharif, H., & Omar, T. (2022). Modeling and Performance Evaluation of an RF Transceiver System at 160 MHz for Railroad Environments. *Proceedings of the 2022 Joint Rail Conference.* ASME.

[70] Ghasemzadeh, P., Hempel, M., Sharif, H., & Omar, T. (2022). An OFDM-Based Transceiver Analysis for Railroad Applications. *022 International Wireless Communications and Mobile Computing (IWCMC)*, *2022*, 748-753.

[71] Ghasemzadeh, P., Hempel, M., & Sharif, H. (2022). A Robust Graph Convolutional Neural Network-Based Classifier for Automatic Modulation Recognition. *2022 International Wireless Communications and Mobile Computing (IWCMC)*, *2022*, 907-912.

Abbreviations and Acronyms

Abbreviation	Definition
3GPP	3rd Generation Partnership Project
AAR	Association of American Railroads
AEI	Automatic Equipment Identification
AMC	Adaptive Modulation and Coding
APSK	Amplitude and phase-shift keying
AREMA	American Railway Engineering and Maintenance-of-Way Association
ATCS	Advanced Train Control System
AWGN	Additive White Gaussian Noise
AWR	Applied Wave Research, Company Name, acquired by Cadence
BS	Base Station
BCH	Bose-Chaudhuri-Hocquenghem, a form of error correction codes
BER	Bit Error Rate
BNSF	Burlington Northern Santa Fa
BPSK	Binary Phase Shift Keying
BR	Bitrate
CFR	Code of Federal Regulations
CORE	Common Open Research Emulator
DCF	Distributed Control Function
DIFS	DCF Inter-Frame Spacing
DQPSK	Differential Quadrature Phase Shift Keying
DTL	Digital Trainline
EM	Electromagnetic
EMI	Electromagnetic Interference
eNB	eNodeB, also evolved Node B
EOTD	End of Train Device
EPC	Evolved Packet Core
ERP	Effective Radiated Power
EVE-NG	Emulated Virtual Environment Next Generation
FCC	Federal Communications Commission
FDTD	Finite-difference time-domain

FEBI	Finite Element - Boundary Integral
FEC	Forward Error Correction
FEM	Finite Element Method
FFT	Fast Fourier Transform
FMN	Frequency Modulation Narrow
FRA	Federal Railroad Administration
FSK	Frequency Shift Keying
FSPL	Free Space Path Loss
FSS	Frequency Structure Simulation
gNB	gNodeB
GNS3	Graphical Network Simulator-3
GUI	Graphical User Interface
HAAT	Height Above Average Terrain
HFSS	High-Frequency Structure Simulation
HOTD	Head of Train Device
IC	Integrated Circuits
IMUNES	Integrated Multi-Protocol Network Emulator/Simulator
ITU	International Telecommunication Union
ITU-T	ITU Telecommunication Standardization Sector
kHz	kiloHertz
LCC	Locomotive Consist Control
LDPC	Low-Density Parity-Check Codes
LMS	Location and Monitoring Service
LOS	Line of Sight
LTCC	Low-Temperature Co-fired Ceramics
LTE	Long-Term Evolution
MS	Mobile
MCS	Modulation and Coding Scheme
MHz	Mega Hertz
MoM	Method of Moments
MRI	Magnetic Resonance Imaging
NEC	Numerical Electromagnetics Code
NF	Noise Figure

NGEC	Next Generation Equipment Committee
NLOS	Non-Line of Sight
NS3	Network Simulator-3
NXDN	Next Generation Digital Narrowband
OFDM	Orthogonal Frequency-Division Multiplexing
OSA	Openairinterface Software Alliance
PAM	Pulse-Amplitude Modulation
PBCH	Physical Broadcast Channel
PCB	Printed Circuit Board
PDCCH	Physical Downlink Control Channel
PDSCH	Physical Downlink Shared Channel
PHY	Physical Layer
PL	Path Loss
PLR	Packet Loss Rate
PRB	Physical Resource Block
PSK	Phase Shift Keying
PTC	Positive Train Control
QAM	Quadrature Amplitude Modulation
QPSK	Quadrature Phase Shift Keying
RB	Resource Block
RCL	Remote-Controlled Locomotive
RF	Radio Frequency
RFIC	Radio-Frequency Integrated Circuit
RFID	Radio Frequency Identification
RX	Receive
SAR	Synthetic-Aperture Radar
SD	Spatial Diversity
SDN	Software Defined Networking
SNR	Signal to Noise Ratio
TAG	Technical Advisory Group
TDL	Tapped Delay Line
TEL	Advanced Telecommunications Engineering Laboratory at UNL
TT	Train Telemetry

TX	Transmit
UNL	University of Nebraska-Lincoln
UCDA	User/Control Plan Decoupled Architecture
UE	User Equipment
USRP	Universal Software Radio Peripheral
VIRL	Virtual Internet Routing Lab
VHF	Very High Frequency
VNX	Virtual Networks over Linux
VNUML	Virtual Network User Mode Linux
WiDTL	Wireless Digital Trainline
XML	eXtensible Markup Language